Astrophysics of star formation across cosmic time with the Square Kilometre Array

GIANFRANCO DE ZOTTI
INAF – OSSERVATORIO ASTRONOMICO DI PADOVA

Layout

- Introduction to the radio sky
- Generalities on radio AGNs
- Radio surveys and their impact on astrophysics and cosmology
- Radio source populations
- Radio emission from star-forming galaxies
- Identification of the faint (sub-mJy) population
- The SKA and the study of the cosmic star-formation history
- Conclusions

The radio sky is very different from that seen in the optical. This composite picture shows how the sky would appear to someone with a "radio eye" 100 m in diameter above an optical photograph of the NRAO site in Green Bank, WV. The radio image is about 45° wide and shows sources down to a flux density limit of ~25 mJy at 4.85 GHz. The extended radio sources concentrated in a band from the lower left to upper right lie in the outer Milky Way. The brightest extended sources are Galactic objects: supernova remnants or HII regions, clouds of hydrogen ionized by luminous stars. Image courtesy of National Radio Astronomy Observatory (NRAO)/Associated Universities Inc. (AUI).

Optical image of the evening sky from Narrabri. Photo by Robin Wark. www.narrabri.atnf.csiro.au/public/sky.html

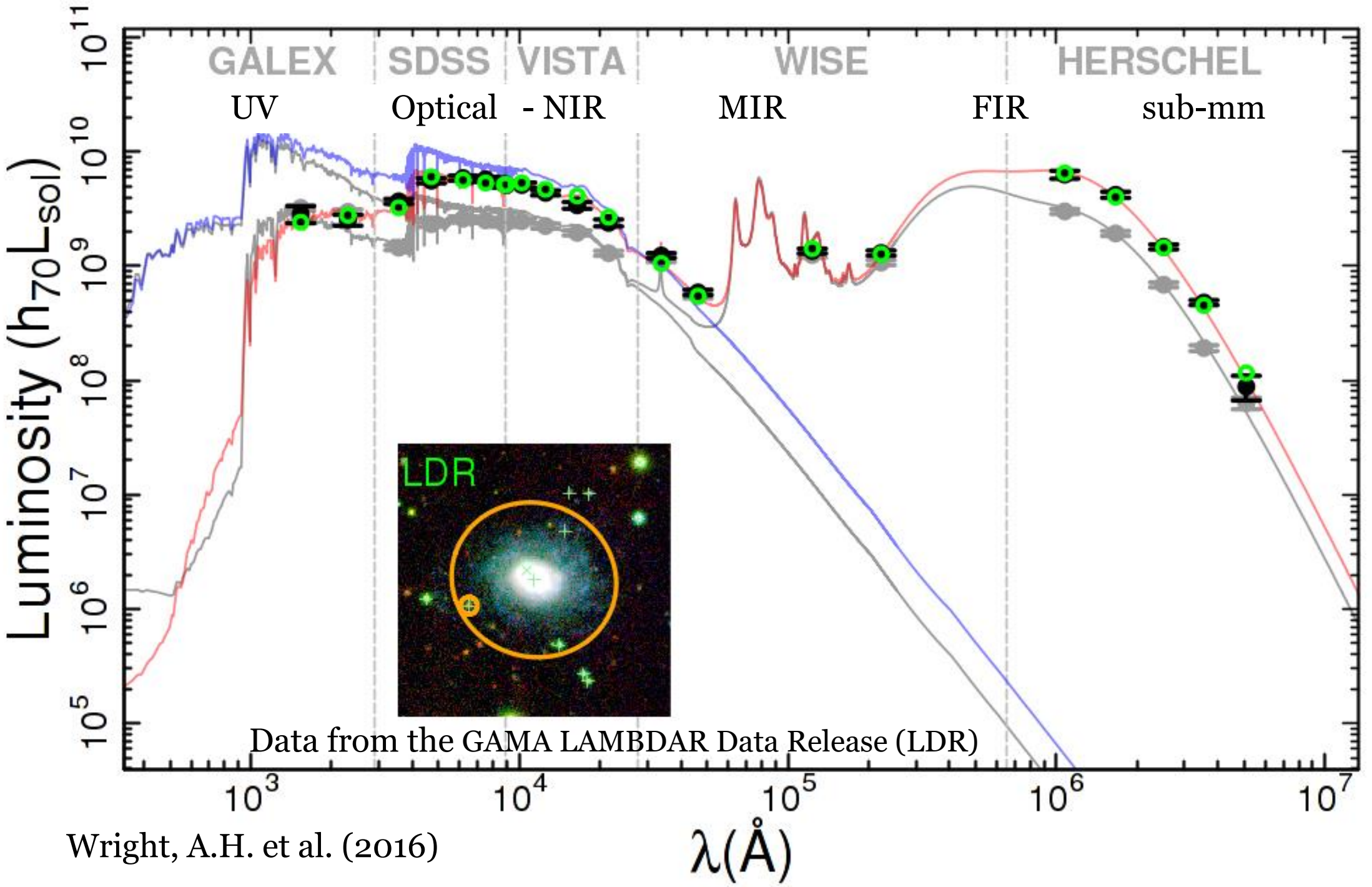

Data from the GAMA LAMBDAR Data Release (LDR)

Wright, A.H. et al. (2016)

AGN Spectral Energy Distribution (SED)

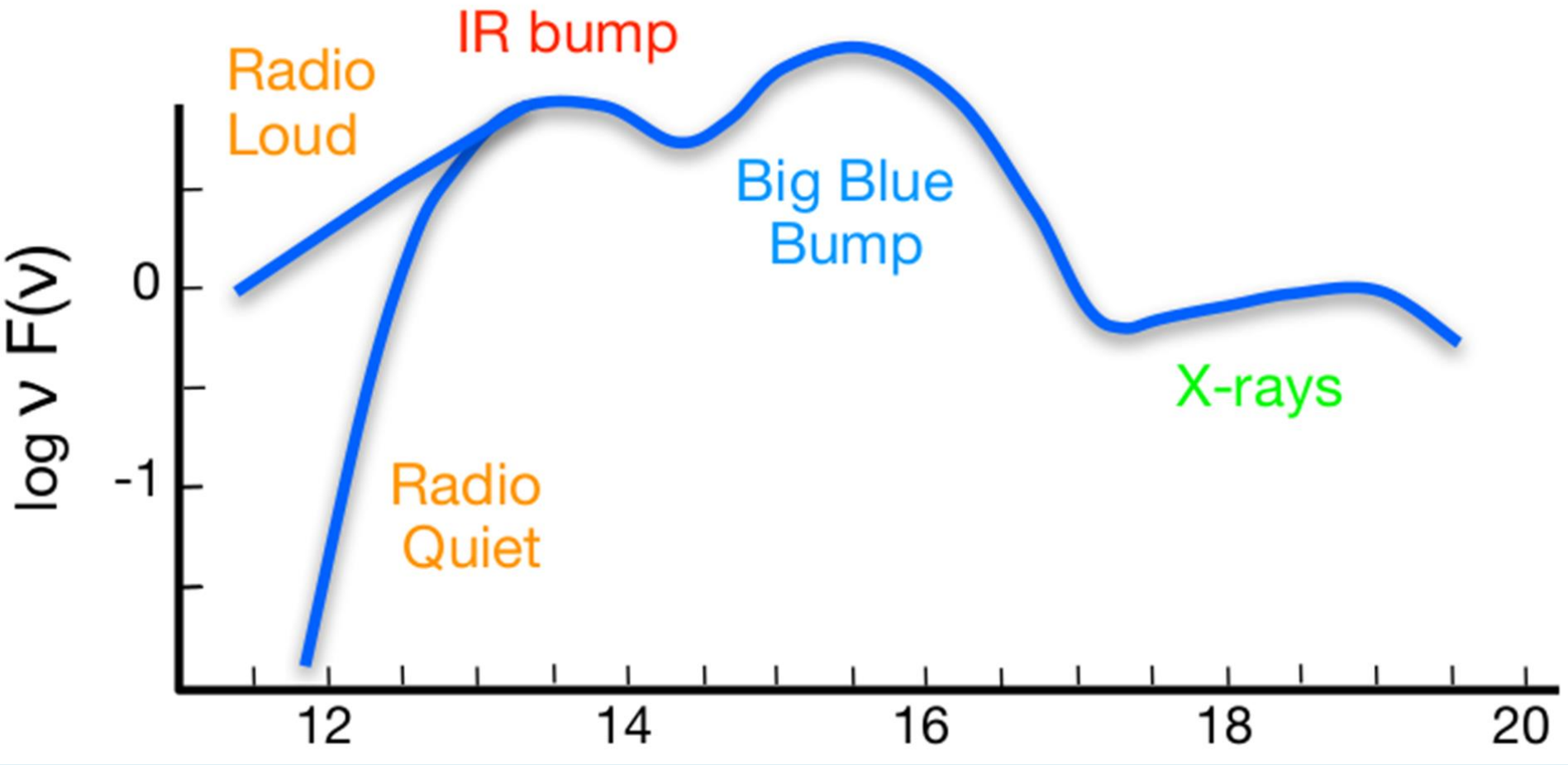

On the contrary, most of the "dots" in the figure, which are unresolved radio sources, are actually distant (median $z \approx 0.8$; Condon, 1989) luminous radio galaxies (RGs) and quasars.

The radio emission from RGs and quasars is *non-thermal*. It is due to ultra-relativistic ($E \gg m_e c^2$) electrons moving in a magnetic field and thereby emitting synchrotron radiation, which, unlike blackbody emission, can cover a very large range in frequency, reaching ~ 10 decades in some sources.

Impact of radio surveys

- The fact that bright radio sources are mostly at substantial redshifts has implied that, for several decades, extragalactic radio surveys remained the most powerful tool to probe the distant universe. Even ‘shallow’ radio surveys, those of limited radio sensitivity, reach sources with redshifts predominantly above 0.5.
- Since the 1960s, the most effective method for finding high-z galaxies has been the optical identification of radio sources, a situation persisting until the mid-1990s, when the arrival of the new generation of 8–10m class optical/infrared telescopes, the refurbishment of the Hubble Space Telescope, the Lyman-break technique (Steidel et al. 1996) and the Sloan Digital Sky Survey (SDSS; York et al. 2000) produced an explosion of data on high-redshift galaxies.
- Indeed radio surveys produced real revolutions in astrophysics and cosmology:

- Radio astronomy first **pushed the boundary of observable universe to cosmological distances**. Ryle and Scheuer (1955) argued that the isotropic distribution of ‘radio stars’ placed the bulk of them beyond 50 Mpc. When arcmin positional accuracy became available (Smith 1952) it was quickly realized that the majority of the host galaxies were beyond the reach of the optical telescopes of the epoch. Minkowski (1960) measured a redshift of 0.46 for 3C295, the redshift record for a galaxy for 10 years. In 1965, the redshift record was 2.0 for the quasar 3C9 (Schmidt 1965). Only after the turn of the century did the redshift record become routinely set by objects discovered in surveys other than at radio wavelengths (e.g. Stern 2000).

- **The discovery of quasars**, starting with 3C273 (Hazard et al. 1963; Schmidt 1963), leading to the picture of the collapsed supermassive nucleus (Hoyle & Fowler 1963), and hence to the now-accepted view of the powerful AGN—massive black-hole+accretion-disk systems (Lynden-Bell 1969) powering double-lobed (Jennison & Das Gupta 1953) radio sources via ‘twin-exhaust’ relativistic beams (Blandford & Rees 1974; Scheuer 1974).

- **The discovery of superluminal motions** of quasar radio components (Cohen et al. 1971), this non-anisotropic emission [anticipated by Rees (1967)] leading to the development of unified models of radio sources: quasars and radio galaxies are one and the same, with orientation of the axis to the viewer’s line of sight determining classification via observational appearance (Antonucci & Miller 1985; Barthel 1989; Urry & Padovani 1995).

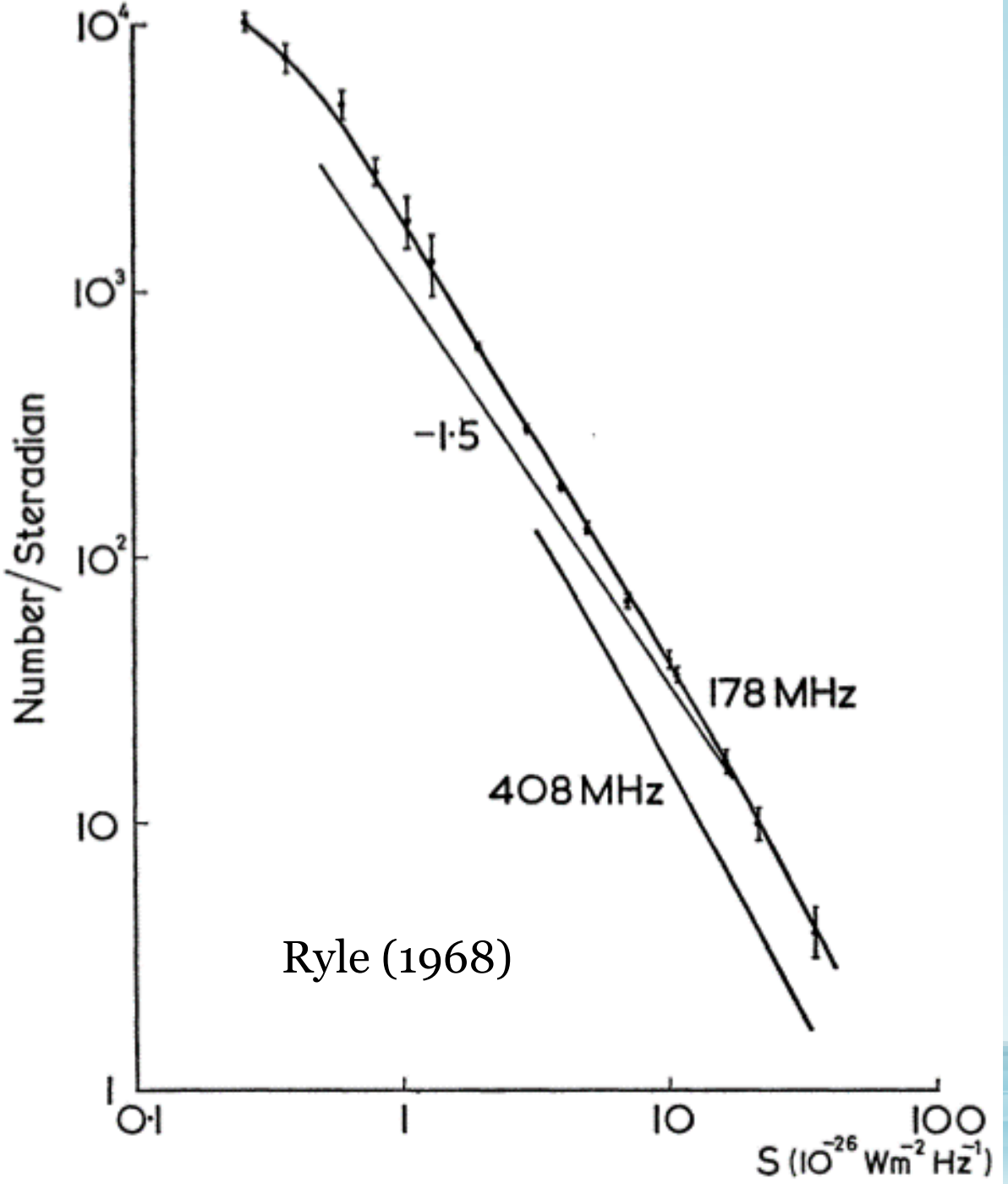

Ryle (1968)

History of the Universe. Early radio surveys highlighted a new global property of the universe: cosmological evolution, disproving the then widely accepted Steady-State model. This achievement was rooted in the simplest statistics to be derived from any survey: the *integral* source counts, the number of objects per unit sky area above given intensities or flux densities. The prediction from the Steady-State, from any reasonable (non-evolving) Friedmann model, or from a static Euclidean universe is that the slope of the cumulative (integral) counts is $-3/2$ [$N(>S) \propto S^{-3/2}$] or flatter. The $-3/2$ slope is the Euclidean case: the number of sources N is proportional to the volume, i.e. to r^3 for a sphere; the flux density is $\propto r^{-2}$, so that $N \propto S^{-3/2}$.

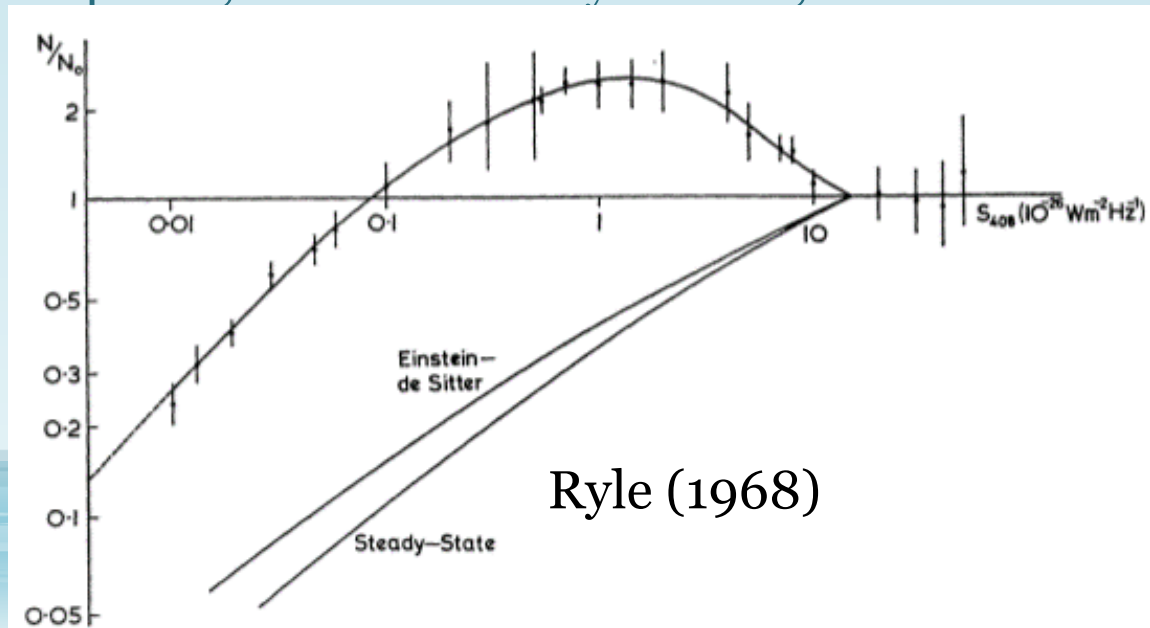

Ryle (1968)

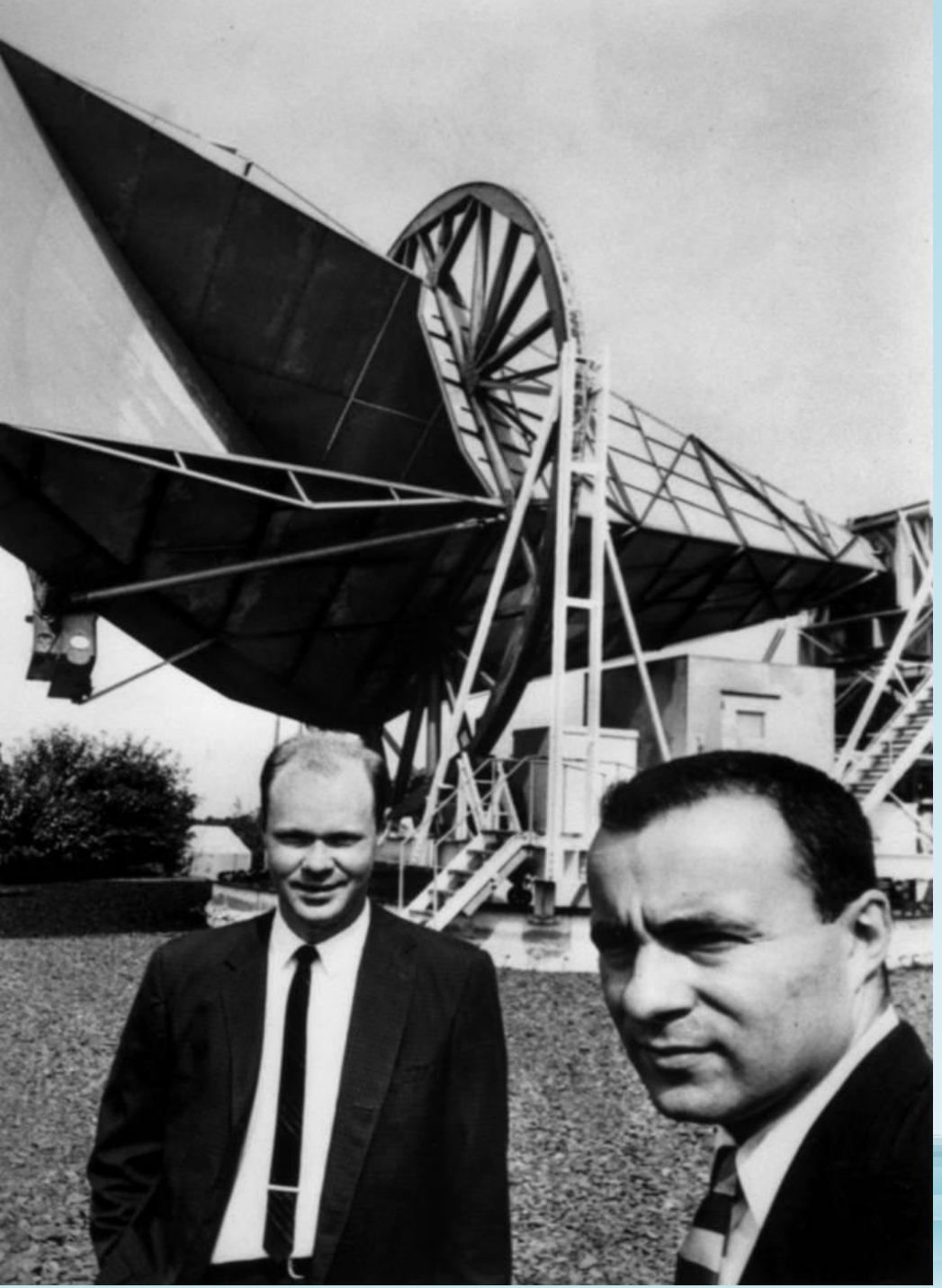

The discovery of the Cosmic Microwave Background (CMB). Penzias and Wilson (1965) found what was immediately interpreted (Dicke et al. 1965) as the relic radiation from a hot dense phase of the Universe. This put the Big Bang model on a firm basis.

Note that while the discovery of the fossil radiation may indeed have shown that a Big Bang took place, definitely ruling out the Steady-State cosmology, the source counts demonstrated further that *objects in the Universe evolve either individually or as a population* — a concept not fully accepted by the astronomy community until both galaxy sizes and star-formation rates were shown to change with epoch.

In the photo Robert Wilson and Arno Penzias with the Holmdel horn antenna, operating at a wavelength λ=7.35 cm, that first detected the CMB.

Discovery of pulsars (Hewish et al. 1968). In 1974 Hewish was awarded the Nobel prize in physics. Observations were done by his student Jocelyn Bell.

Discovery of the first pulsar in a binary system (Hulse & Taylor 1975), allowing tests of general relativity in a strong gravitational field. Such a compact system with rapidly orbiting masses would radiate large quantities of gravitational radiation. Taylor monitored the pulsar system for decades, finding that the shift of the periastron time is in close agreement with predictions from general relativity. Russell Hulse and Joseph Taylor were awarded the Nobel Prize 1993.

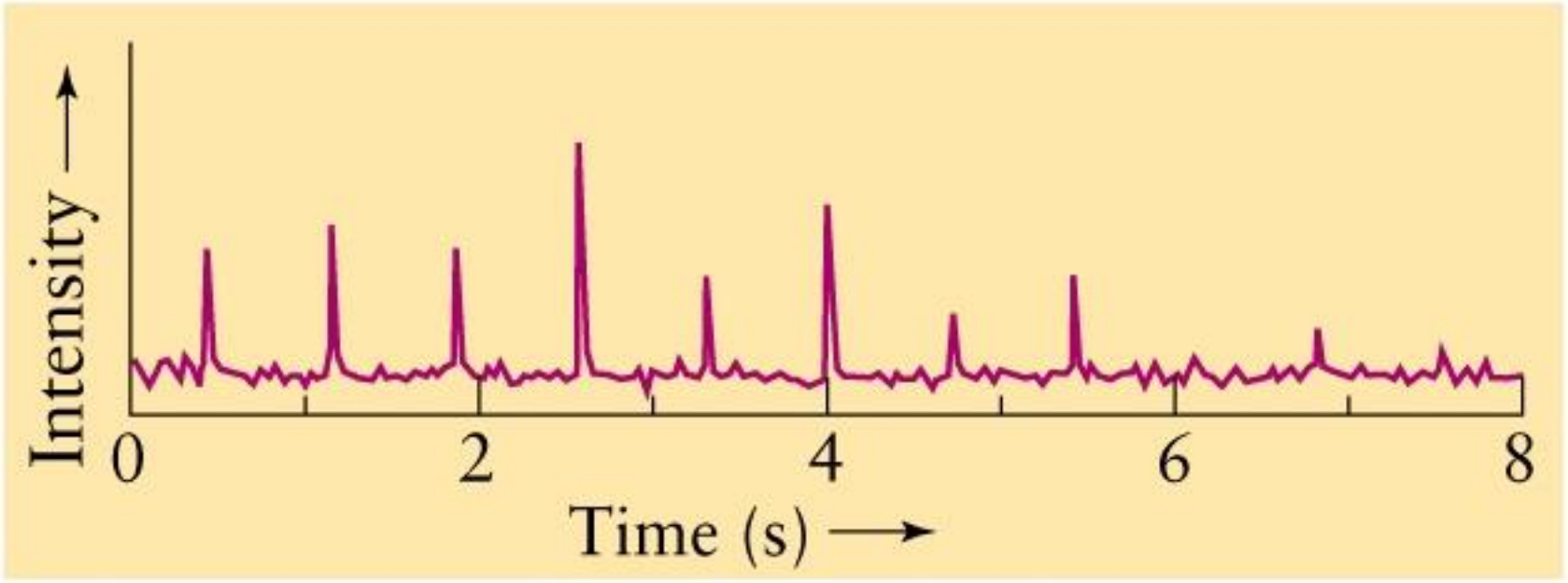

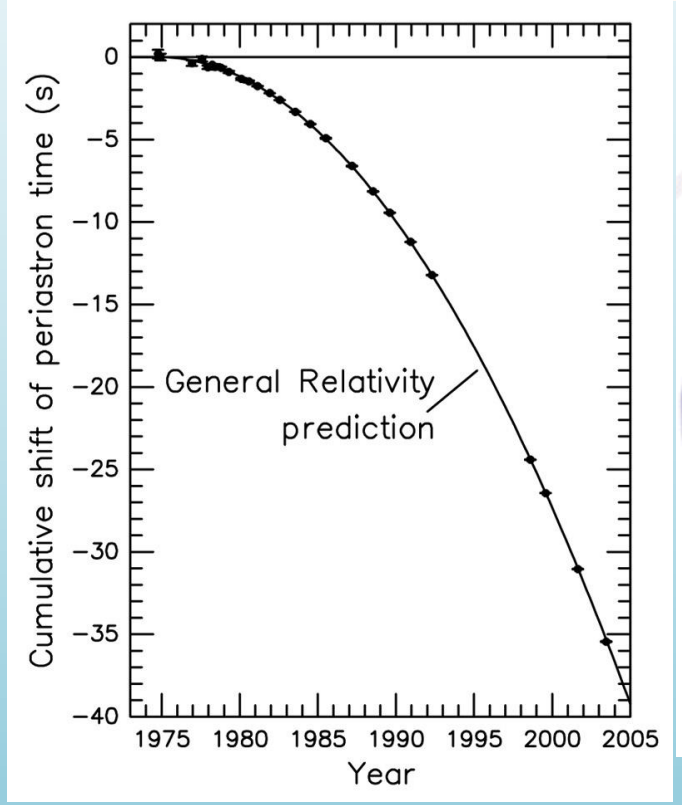

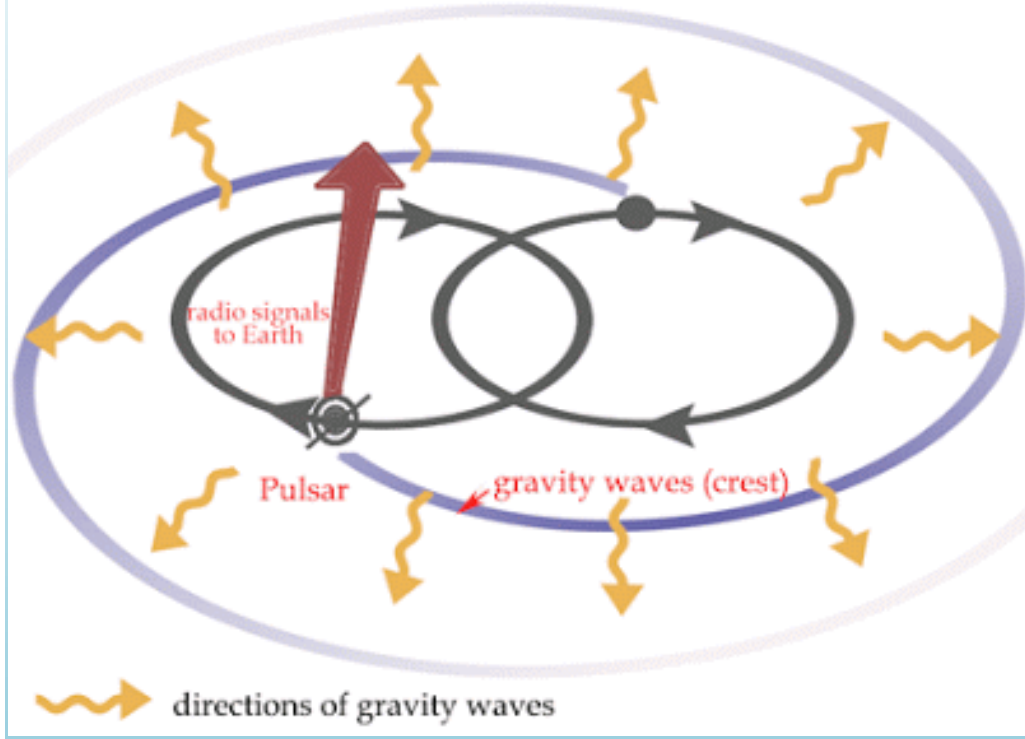

Source counts

- Source counts are currently recognized as essential data in delineating the different radio-source populations and in defining the cosmology of AGNs.
- These counts are dominated down to milli-Jansky (mJy) levels by the canonical radio sources, believed to be powered by supermassive black-holes (e.g. Begelman et al. 1984) in AGNs. (The standard flux density unit in radio astronomy is the Jansky (Jy), 1 Jy= 10^{-23} erg cm^{-2} s^{-1} Hz^{-1} = 10^{-26} W Hz^{-1}. By today's standards strong radio sources have $S_\nu \geq 1$ Jy, intermediate ones have 1 mJy $\leq S_\nu <$ 1 Jy, while weak radio sources are below the mJy (soon μJy) level).
- *Unified models* provide a framework for a discussion of such sources. According to the widely accepted 'unification' scheme (Scheuer & Readhead 1979; Orr & Browne 1982; Scheuer 1987; Barthel 1989), the appearance of sources steep-spectrum/flat-spectrum dichotomy, depends primarily on their axis orientation relative to the observer. This paradigm stems from the discovery of relativistic jets (Cohen et al. 1971; Moffet et al. 1972) giving rise to strongly anisotropic emission.

Radio quasars and RGs are somewhat rare, mostly non-thermal sources across the entire electromagnetic spectrum, in which a large fraction of the total emission comes from relativistic jets, that is streams of plasma with speeds getting close to the speed of light, and associated lobes.

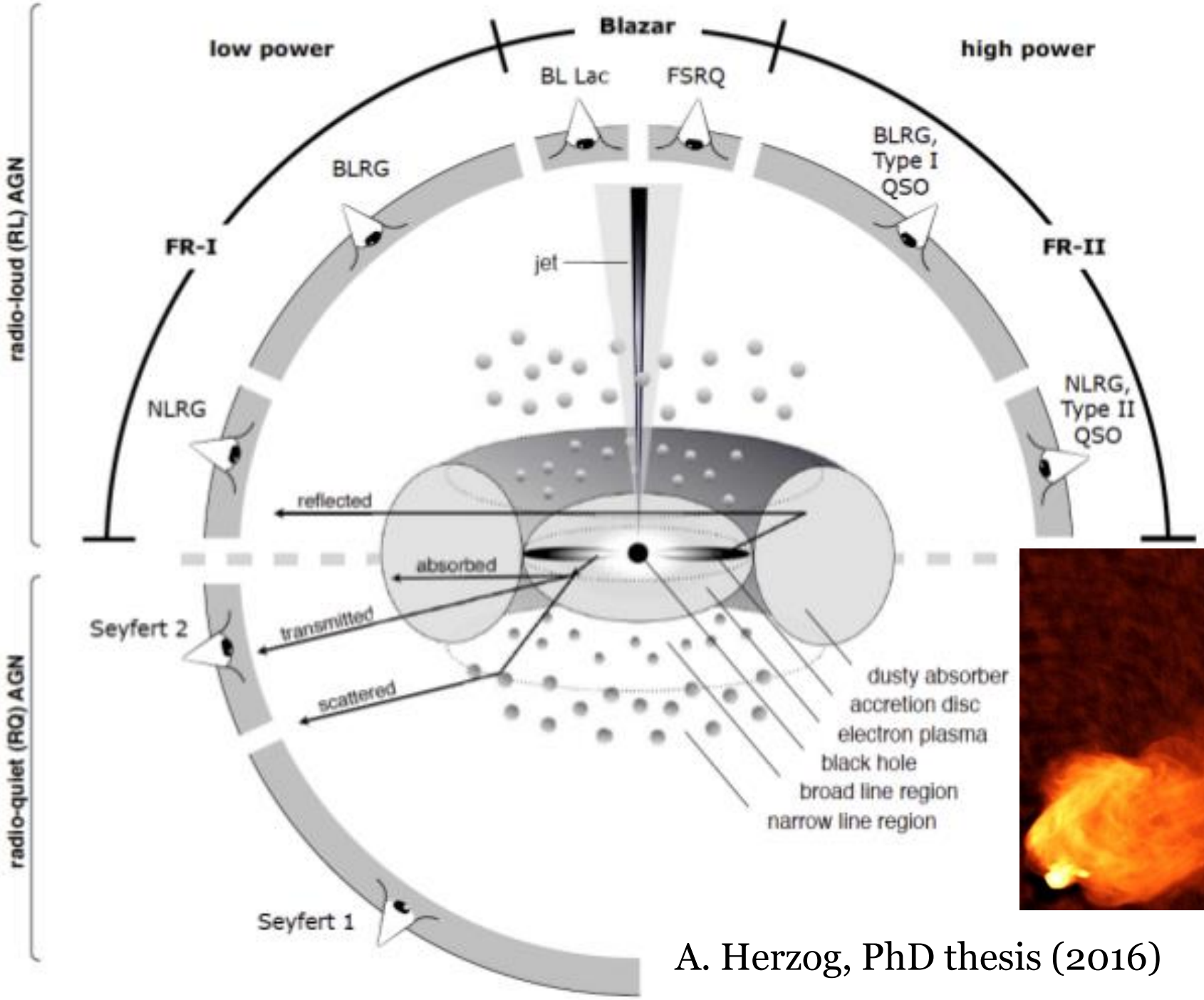

A. Herzog, PhD thesis (2016)

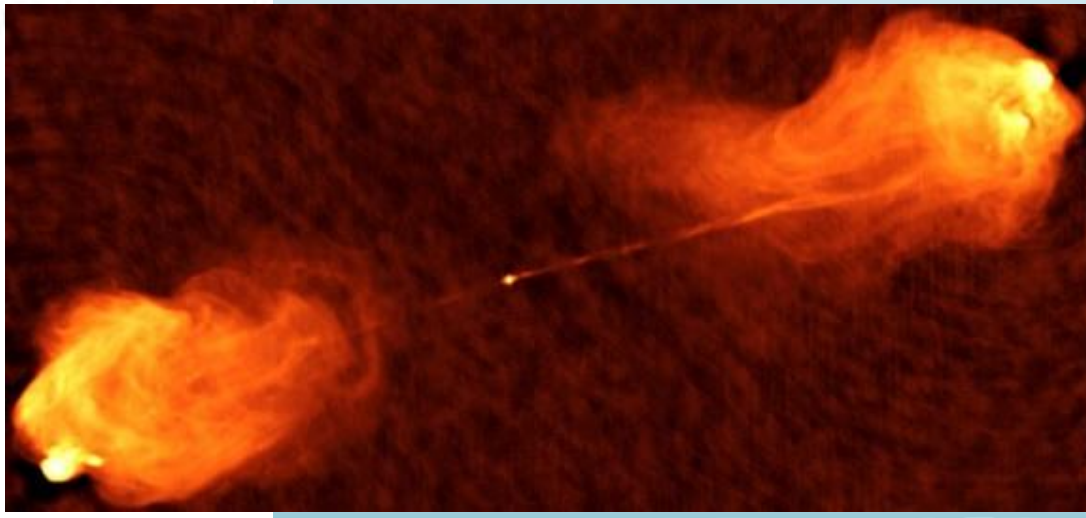

Cygnus A. Image courtesy of NRAO/AUI

Unification scheme

- A line of sight close to the source jet axis offers a view of the compact, Doppler-boosted, flat-spectrum base of the approaching jet. Doppler-boosted low-radio-power [Fanaroff & Riley 1974, type I (FRI; edge-dimmed)] sources are associated with BL Lac objects, characterized by optically featureless continua, while the powerful type II (FR II; edge-brightened) sources are seen as flat-spectrum radio quasars (FSRQs). Flat-spectrum means an average spectral index $\alpha < 0.5$ ($S_\nu \propto \nu^{-\alpha}$); typically $\alpha \sim 0$.
- The view down the axis offers unobstructed sight of the active nucleus which may outshine the starlight of the galaxy by five magnitudes. The source appears stellar, either as a FSRQ or as a BL Lac object. FSRQs and BL Lacs are collectively referred to as *blazars*.
- In the case of a side-on view, the observed low-frequency emission is dominated by the extended, optically thin, steep-spectrum components, the radio lobes; and the optical counterpart generally appears as an elliptical galaxy. A dusty torus (Antonucci & Miller 1985) hides the active nucleus emission from our sight. Steep-spectrum sources typically have spectral index $\alpha \approx 0.75$.
- At intermediate angles between the line of sight and the jet axis, angles at which we can see into the torus, but the alignment is not good enough to see the Doppler-boosted jet bases, the object appears as a ‘steep-spectrum quasar’.

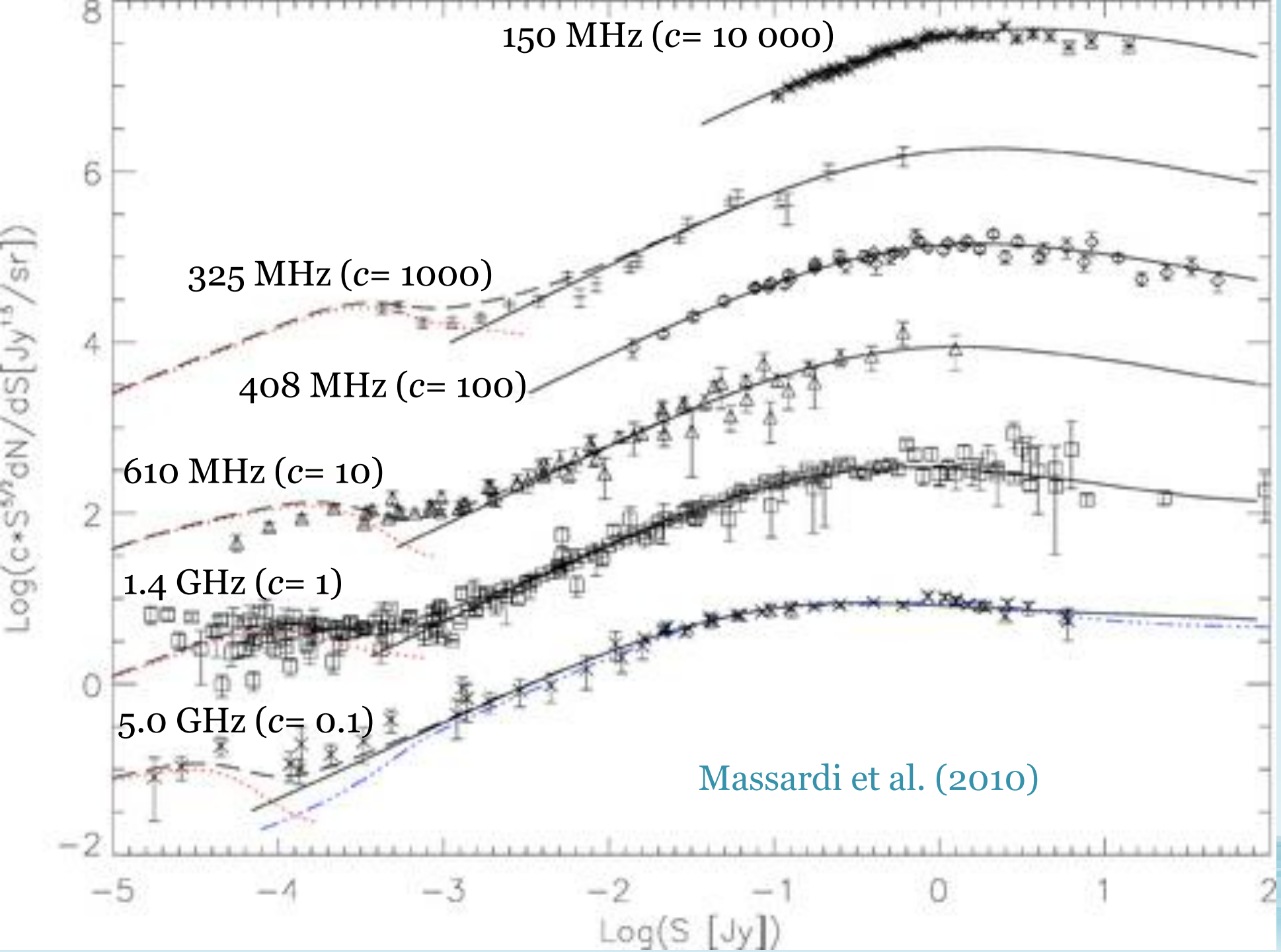

Observed Euclidean-normalized number counts.

Counts down to mJy levels are accounted for by radio-loud AGNs. But when radio surveys reached sub-mJy flux density levels (Windhorst et al. 1984; Condon & Mitchell 1984), the Euclidean normalized counts showed a flattening or an upturn, indicative as the emergence of a new population.

The faint radio source population

- Windhorst et al. (1985), based on optical identifications available for less than half of the sample, suggested that "for $1 < S\,1.4 < 10$ mJy a blue radio galaxy population becomes increasingly important; these often have peculiar optical morphology indicative of interacting or merging galaxies".
- The identification by Kron et al. (1985) showed that "For $18.5 \leq V \leq 21.5$, about one-third of the mJy radio galaxies are bluer than the giant ellipticals. They are not morphologically like the brighter spirals, but rather are a different class of peculiar (interacting, merging, or compact) galaxies".
- Danese et al. (1987) showed that evolving starburst/interacting galaxies could easily account for the excess counts, for observed colours and morphological properties. On the contrary, the data could not be interpreted in terms of a new population of unevolving low-luminosity radio sources or of normal spiral galaxies with evolution consistent with the observational constraints.
- However, to really understand which sources were responsible for the flattening and sort out the source population of the ≤ 1 mJy radio sky took more than thirty years.

The local radio luminosity function

The local radio luminosity function has contributions from two populations. The bright portion ($P_{1.4GHz} \geq 10^{23}$ W Hz^{-1}) is dominated by canonical, steep-spectrum radio galaxies (RGs), whose luminosities reach $P_{1.4GHz} \approx 10^{24}$ W Hz^{-1}.

At lower luminosities star-forming galaxies (SFGs) take over. Luminosities of reach only $P_{1.4GHz} \approx 10^{24}$ W Hz^{-1} (Sadler et al., 2002; Mauch & Sadler, 2007).

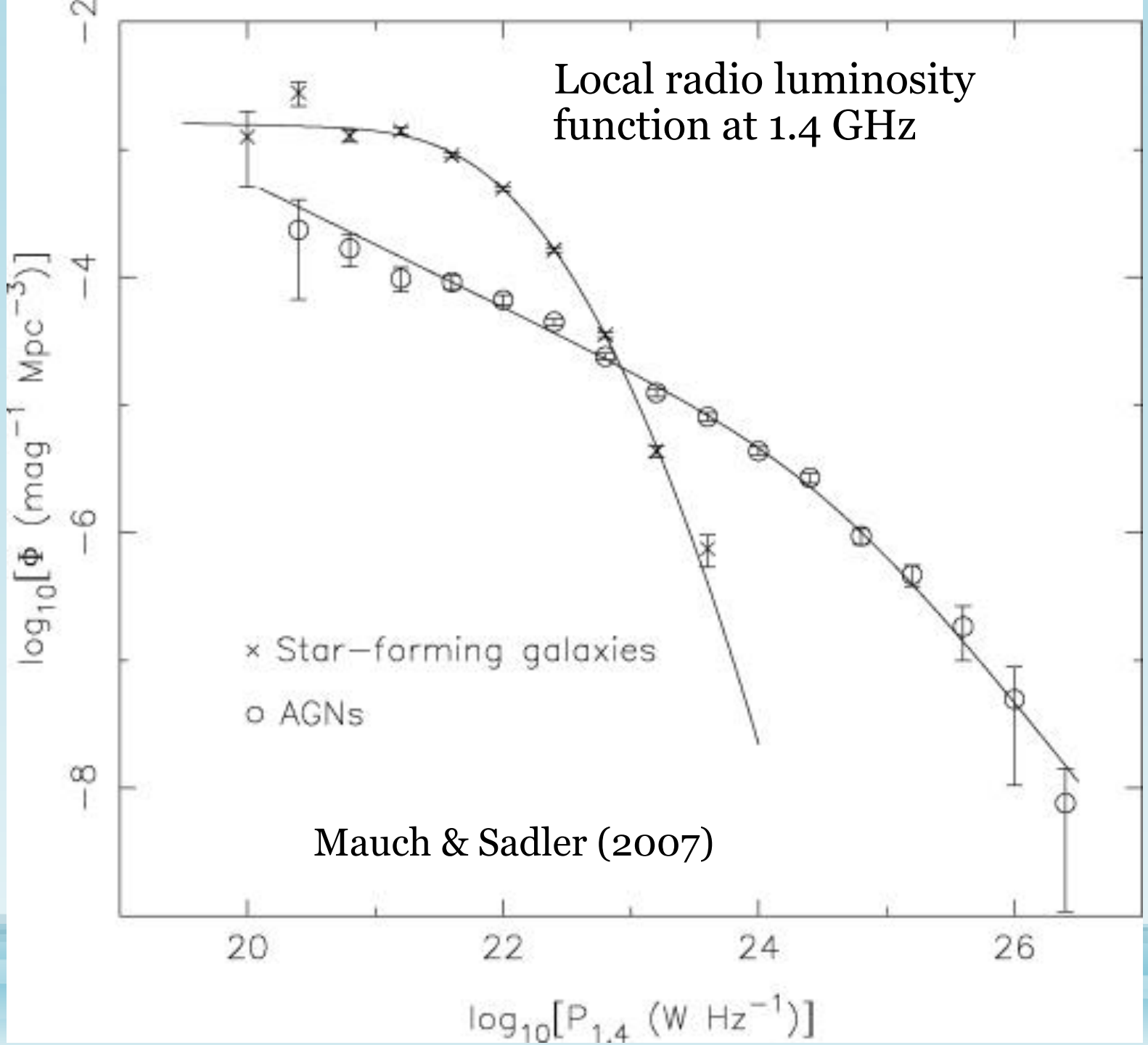

Radio emission of star-forming galaxies (SFGs) - 1

- Unlike RGs, where the ultimate prime mover is the central black hole, the radio emission of SFGs is related to star-formation and has two components: synchrotron radiation from relativistic electrons and free-free emission from H II regions.
- The synchrotron emission results from relativistic plasma, thought to be accelerated primarily in supernova remnants (SNRs) associated with massive (mass larger than about 8 $M_{\odot}$) stars that end as Type II and Type Ib supernovae. Such massive stars live $\leq 3 \cdot 10^7$ yr, and the relativistic electrons probably have lifetimes $\leq 10^8$ yr (Condon 1992).
- Thus the relativistic electrons emitting the synchrotron radiation have propagated significant distances (≥ 1 kpc) from their short-lived ($\geq 10^5$ yr) and now defunct parent SNRs. Consequently the original sources of the relativistic electrons have disappeared, and their detailed spatial distribution has been smoothed beyond recognition (Condon 1992).
- Moreover, the steps between star formation and synchrotron emission (supernova explosion, acceleration of relativistic electrons in the SNR, propagation of cosmic rays throughout the galaxy, energy loss, and escape) are poorly understood, impeding quantitative interpretation of the observed synchrotron spectra and brightness distributions.

Radio emission of star-forming galaxies (SFGs) - 2

- However there is a remarkably tight and ubiquitous correlation between the global far-IR (FIR) and the (predominantly synchrotron) radio luminosities of star forming galaxies.
- Except for galaxies with very low star-formation rates, the FIR luminosity appears to be a good measure of the bolometric luminosity produced by massive ($M \geq 5\ M_{\odot}$) young stars which are the most efficient dust heaters.
- Hence, also the synchrotron luminosity can be safely exploited as a measure of the star formation rate (SFR).
- In the figure, the gray filled circles identify the radio-excess objects, with nuclear radio emission. The remaining ~1750 objects (out of 1809) lie very close to the linear relation, and the rms scatter of the data is less than 0.26 dex.

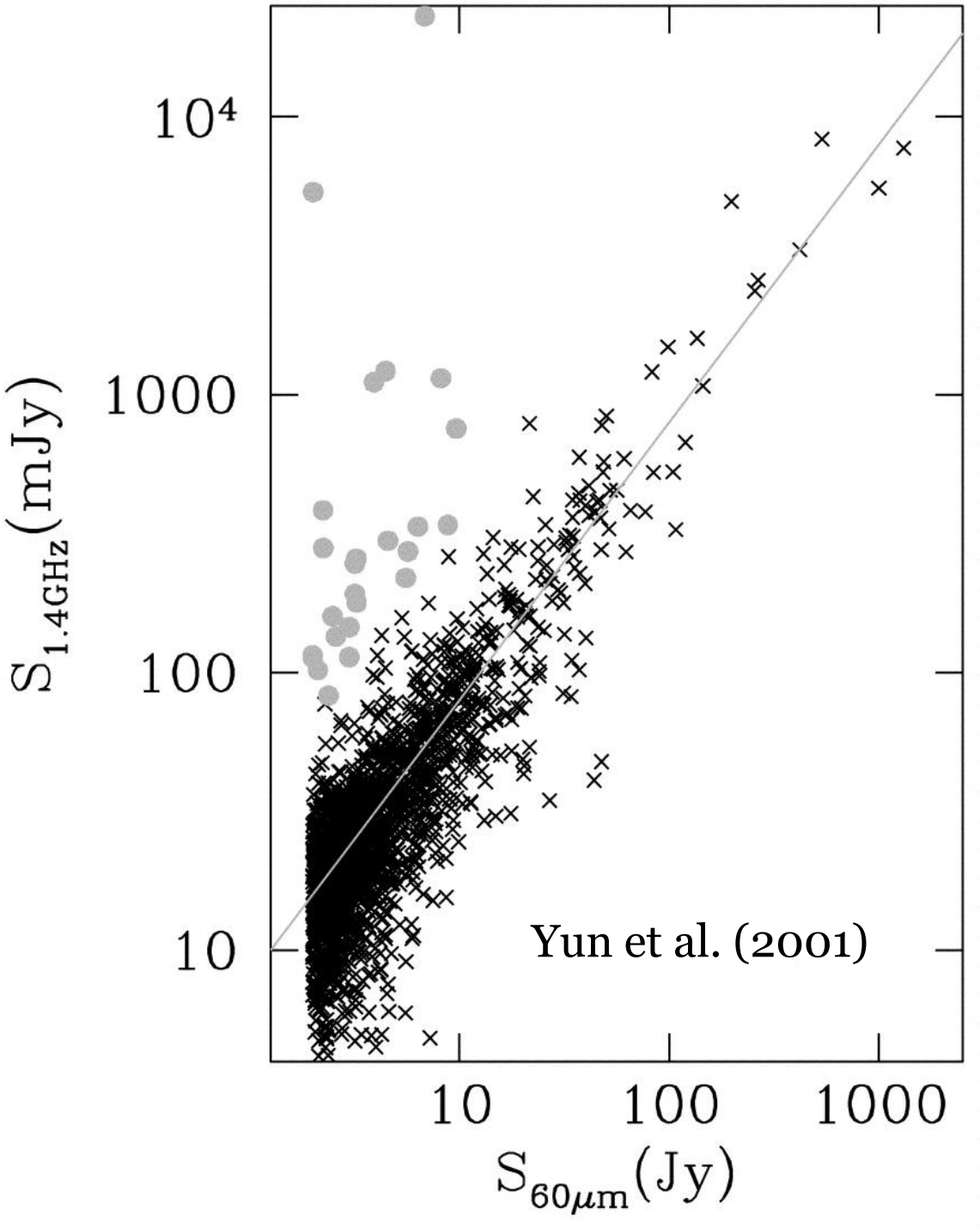

The radio-FIR correlation persists up to high redshifts (Ivison et al. 2010, Magnelli et al. 2015; Delhaize et al. 2017).

The figure shows the total IR (TIR; 8-1000 μm) versus 1.4 GHz luminosity for star-forming objects in the ultra-deep 3 GHz COSMOS survey to an average sensitivity of 2.3 μJy beam^{-1} and including galaxies up to $z \sim 5$.

Black points : objects detected in both the radio and infrared data; red arrows: objects in the radio-detected sample with upper limits in the infrared; blue arrows: objects in the infrared-detected sample with upper limits in the radio. The red points correspond to objects with radio excess, attributed to nuclear activity.

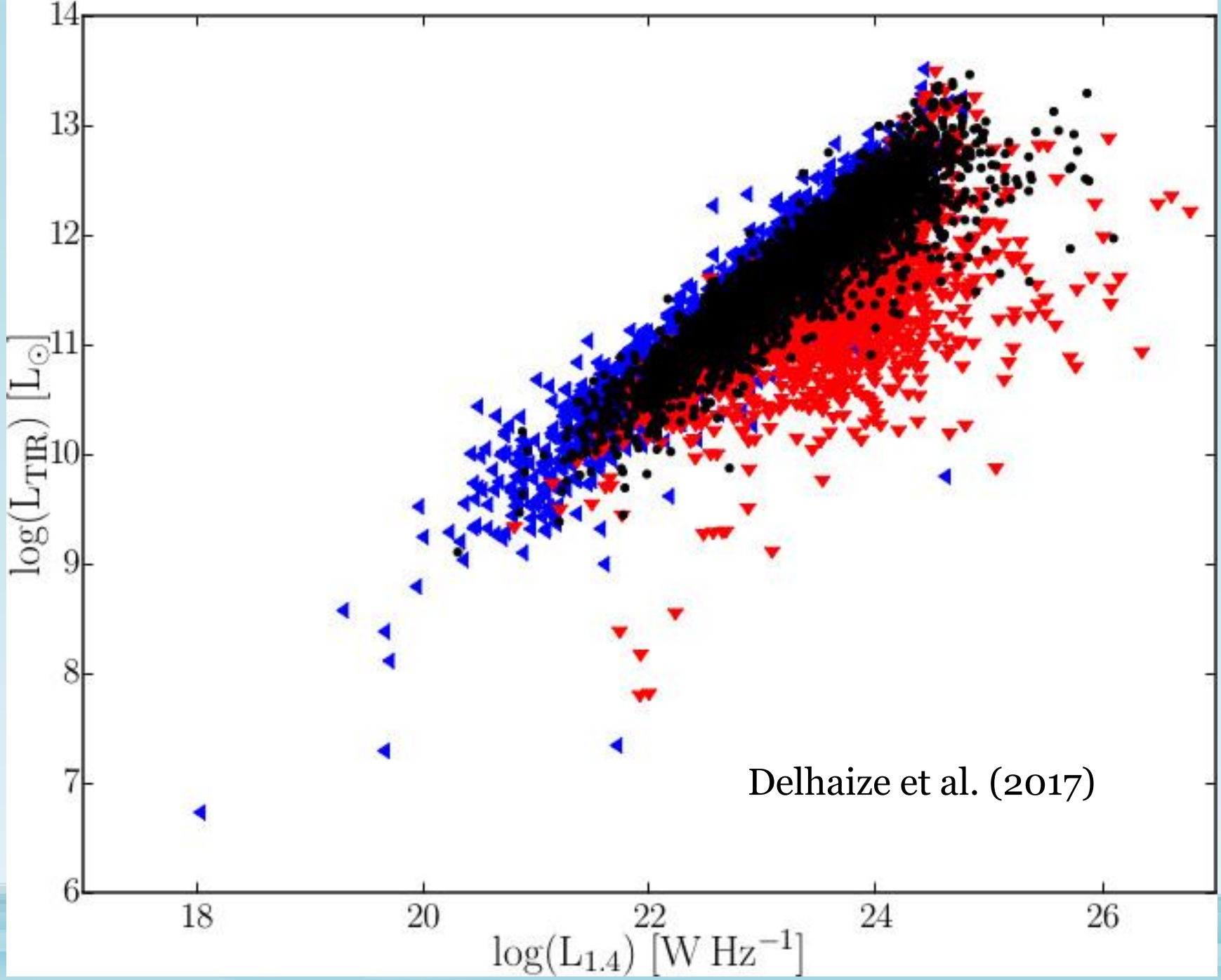

Delhaize et al. (2017)

Radio emission of star-forming galaxies (SFGs) - 3

- The massive stars ionize the HII regions as well and therefore power the free-free emission whose intensity is therefore proportional to the production rate of Lyman continuum photons.
- Thus, the free-free emission: i) would allow the mapping of star-formation regions even in deeply dust-enshrouded regions; ii) is a measure of the instantaneous star formation rate, while the information from the synchrotron is delayed by $\geq 10^7$ yr.
- Radio maps can be made with sub-arcsec position accuracy and resolution, unambiguously identifying the most luminous star-forming regions within galaxies and resolving even the most compact ones.
- At radio wavelengths also the densest star-forming regions, generally associated to the most intense starbursts, are transparent, so that observed flux densities are accurately proportional to intrinsic luminosities.
- Radio stars are rare; therefore their contamination of emission from star-forming regions is generally negligible.

Radio emission of star-forming galaxies (SFGs) - 4

- Synchrotron, with a spectral index $\alpha \approx 0.7$-0.8 ($S \propto \nu^{-\alpha}$), generally dominates at rest-frame frequencies ≤ 30 GHz, and above ~ 100 GHz the radio emission is overwhelmed by re-radiation of thermal dust, heated by young stars. Hence, the free-free emission, which has an effective spectral index at radio frequencies $\alpha \approx 0.1$, emerges only over a narrow frequency range: isolating it and measuring its flux density is observationally difficult.
- Note however the timescales. Most of the synchrotron radiation in a typical galaxy arises from fairly old ($\geq 10^7$ yr) relativistic electrons. Hence, the radio emission in the youngest galaxies should be free-free. This is expected to be particularly relevant at the highest redshifts, when cosmic timescales are short.

Radio emission of star-forming galaxies

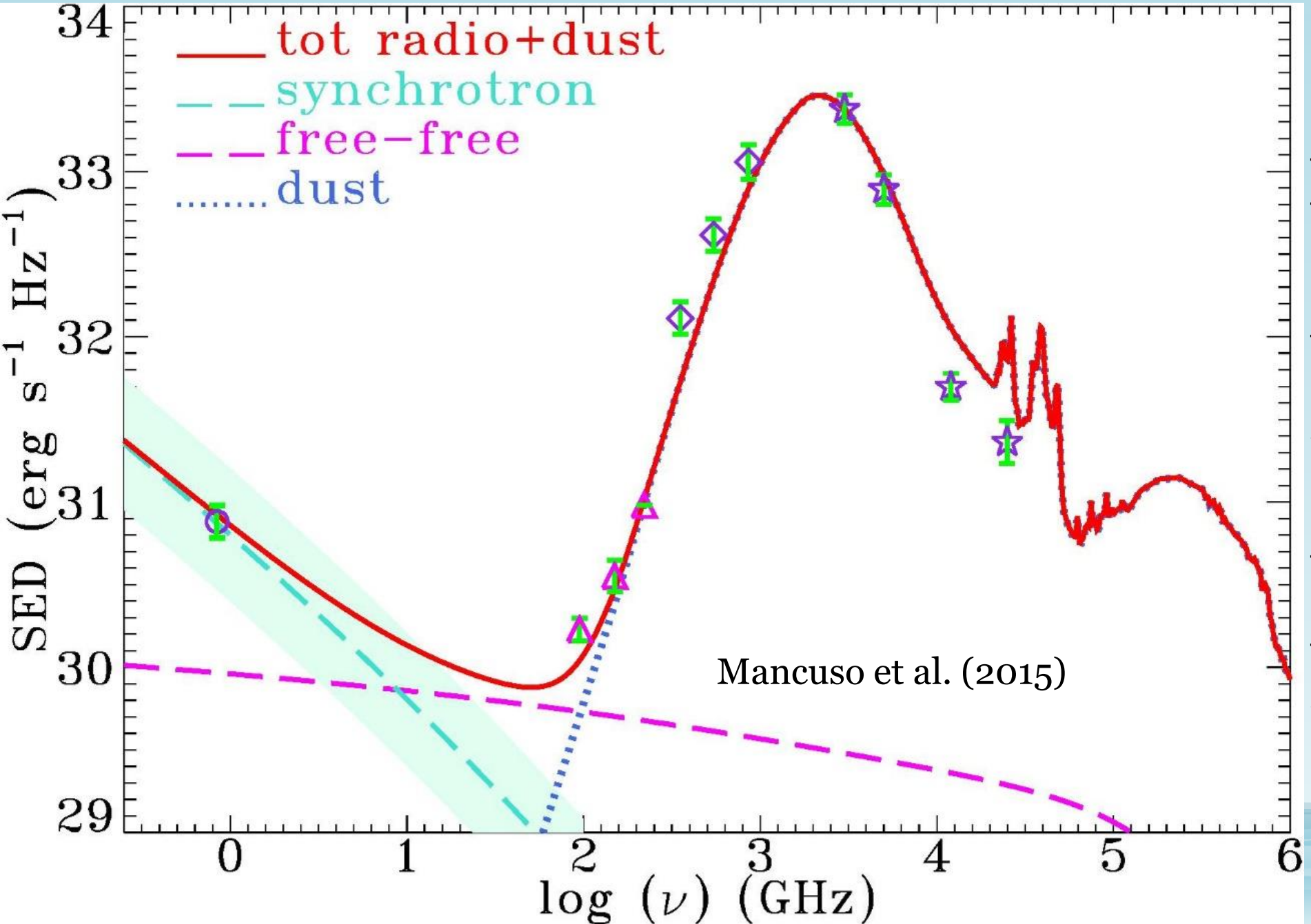

SED of the star-forming galaxy SPT-SJ213629-5433-4. The red curve is a fit made by eye summing the Cai et al. (2013) SED of a cold late-type galaxy (dotted blue line**)** with the free–free (long-dashed magenta line) and the synchrotron emission corresponding to the same SFR. Data points: radio flux densities from the NED (open circles); SPT flux densities (triangles); *Planck* flux densities (open diamonds); IRAS flux densities (open stars).

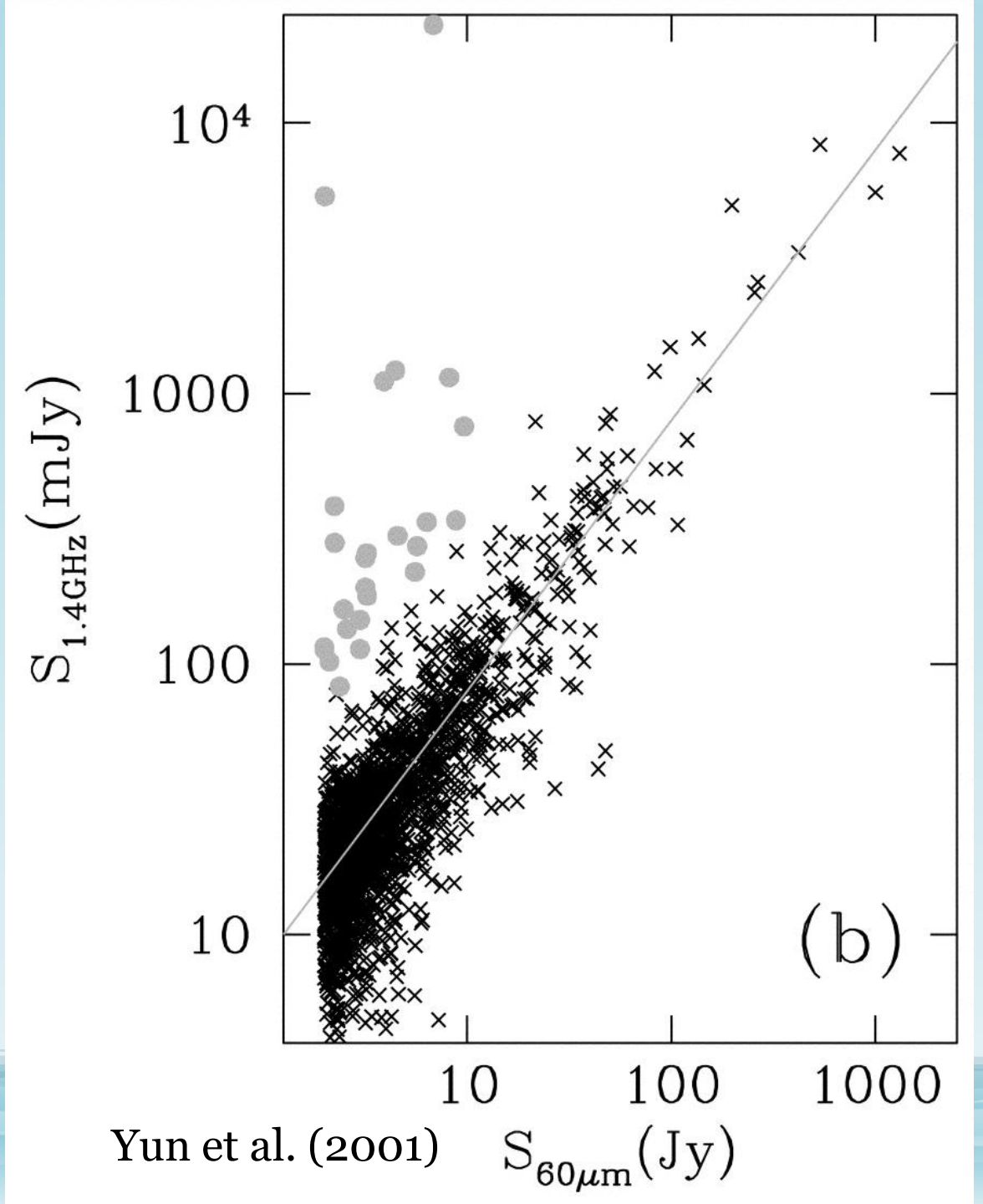

Yun et al. (2001)

Synchrotron luminosity at low SFRs

- However, it has long been suggested that the synchrotron radiation from low SFR galaxies is somewhat suppressed (Klein et al. 1984; Chi & Wolfendale 1990; Price & Duric 1992), although this view was controversial (Condon 1992).
- A convincing argument in this direction was made by Bell (2003). He pointed out that the FIR emission traces most of the SFR in luminous star-forming galaxies but only a minor fraction of it in faint galaxies, as demonstrated by the fact that they are mostly blue, implying that only a minor fraction of the light from young stars is absorbed by dust. Nevertheless the FIR to radio luminosity ratio is similar for the two galaxy groups, implying that the radio emission from low-luminosity galaxies is substantially suppressed, compared to brighter galaxies.
- A plausible physical region for the suppression of synchrotron emission of low luminosity galaxies is that these galaxies are unable to confine relativistic electrons. They can then escape into the intergalactic medium before releasing their energy via synchrotron emission.
- A direct test of the L_{sync} vs SFR relation can be made comparing the observational determinations of the local SFR function (Mancuso et al. 2015; Aversa 2015) with that of the local radio luminosity function (Mauch & Sadler 2007).

Test of the synchrotron luminosity – SFR relation - 1

- A suppression of the synchrotron luminosity is also expected at high frequencies because of the “electron ageing” effect.
- A further damping of synchrotron emission may be expected at high z because of the increase of inverse Compton energy losses off the CMB photons whose energy density goes as $(1+z)^4$.
- On the other hand, Magnelli et al. (2015), based on FIR and radio observations of the most extensively studied extragalactic fields (GOODS-N, GOODS-S, ECDFS, and COSMOS) reported evidence of a weak redshift evolution of the parameter $q_{FIR}=\log[L_{FIR}\ (W)/3.75\times10^{12}]-\log(L_{1.4\ GHz}/\ W/Hz)$. They found

$$q_{FIR}=2.35\pm 0.08)\times (1+z)^{\alpha M}, \text{ with } \alpha M = -0.12\pm 0.04.$$

- The weak but statistically significant trend of q_{FIR} with redshift has been recently confirmed by Delhaize et al. (2017) up to $z \approx 5$.

Test of the synchrotron luminosity – SFR relation - 2

- The evolution of q_{FIR} reported by Magnelli et al. (2015) implies an increase with redshift of the L_{synch}/SFR ratio:

$$\log[L_{synch,1.4GHz}(z)]=\log[L_{synch,1.4GHz}(0)] +2.35[1-(1+z)^{-0.12}].$$

- This is in contradiction with expectations from inverse Compton cooling of relativistic electrons at high redshifts (but this effect should show up primarily at high frequencies).

- On the other hand, a decrease in q_{FIR} with redshift was expected by some of the most up-to-date theoretical models (e.g. Lacki et al. 2010, Lacki & Thompson 2010, Schleicher & Beck 2013) because of the increase with redshift of the SFR surface density and of the gas density that may better confine relativistic electrons; the magnetic field may also be amplified.

Test of the synchrotron luminosity – SFR relation - 3

- However, the precise mechanism accounting for the radio FIR correlation, including the evolution of q_{FIR} is not well understood, yet.
- A direct test of the L_{sync} vs SFR relation, made comparing the observational determinations of the SFR function and of the radio luminosity function, now available up to high redshifts has been carried out by Bonato et al. (2017.

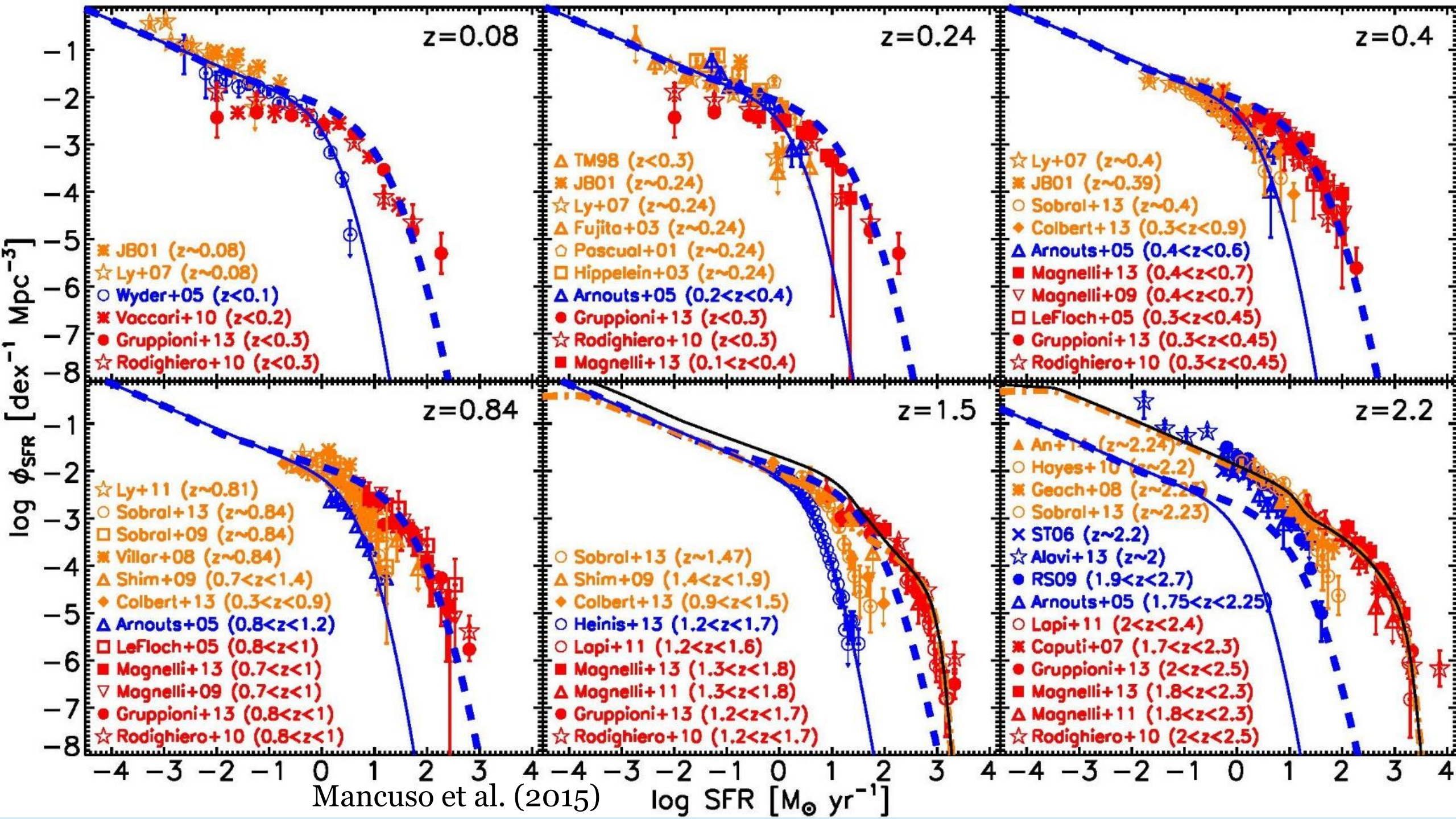

Mancuso et al. (2015)

Determinations of the SFR function need to take into account both the unobscured and the dust-obscured star formation. At high SFRs, the star formation is almost completely dust-obscured and can be measured via FIR/sub-mm observations. At low SFR, most star-formation is unobscured and can be measured via optical/UV observations both in the continuum or in emission lines (primarily Lyα and Hα).

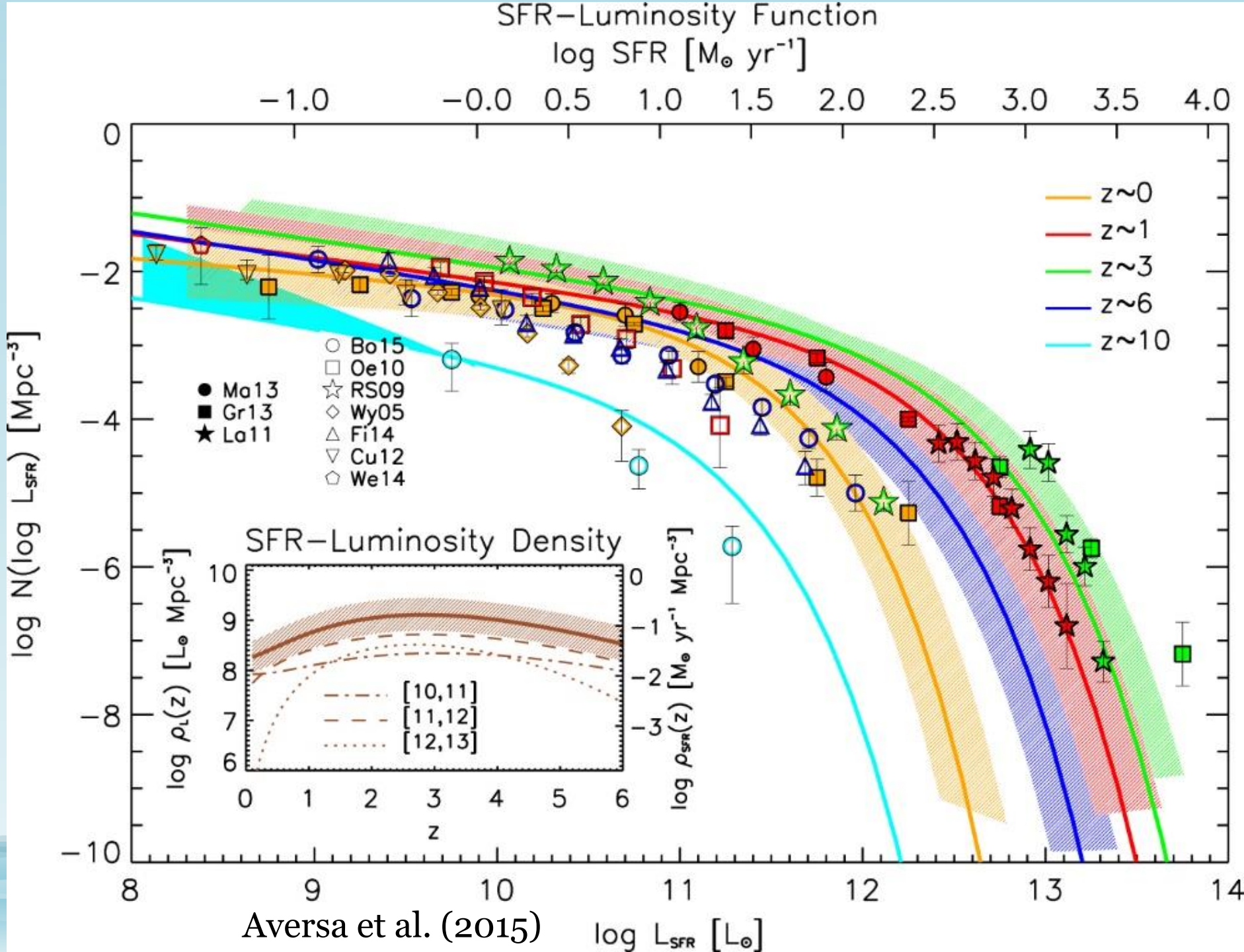

Aversa et al. (2015)

The conversion of the local SFR function into the local radio luminosity function (LF) using the Murphy et al. (2011) calibration (dot-dashed line) over-predicts the low luminosity portion of the Mauch & Sadler (2007) local LF at 1.4 GHz (data points) and under-predicts its bright portion. This discrepancy was previously pointed out by Massardi et al. (2010).

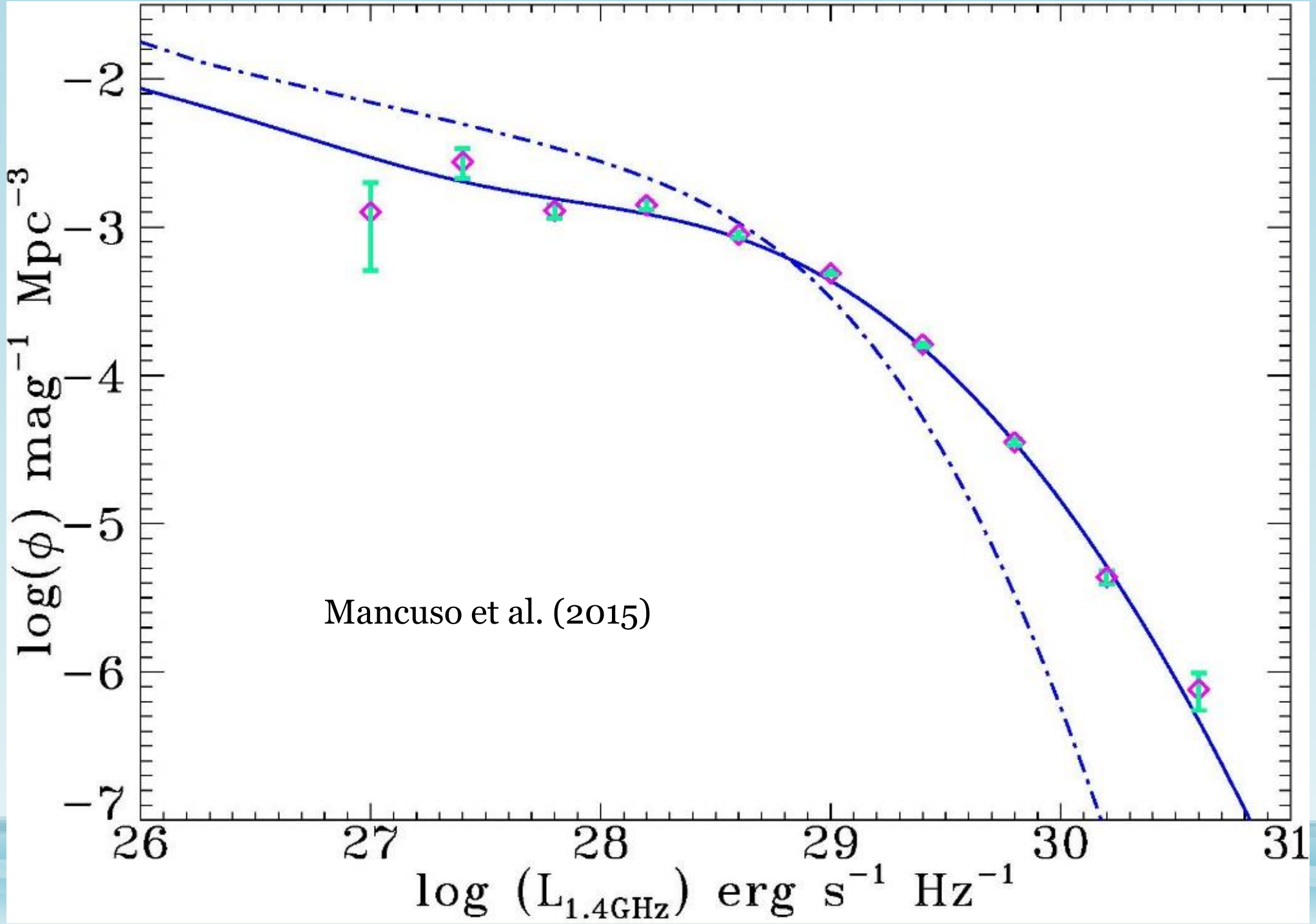

The figure (from Bonato et al. 2017) compares the 1.4 GHz radio luminosity functions (RLFs) obtained from the SFR functions with observational determinations at several redshifts up to z≈5.

The solid blue lines assume no evolution of q_{FIR} while the dark brown solid lines take into account the the best-fit evolution of the mean L_{synch}/SFR ratio from Magnelli et al. (2015).

Also shown, for comparison, are two phenomenological parameterizations of the RLF (Smolčić et al. 2009): the Condon (1989, 'Condon' model, dashed cyan lines) and the Sadler et al. (2002, 'Sadler' model, orange short dashes) parameterizations of the RLF.

The luminosity function data are consistent with a moderate increase of the L_{synch}/SFR ratio with increasing redshift, although a constant ratio cannot be ruled out.

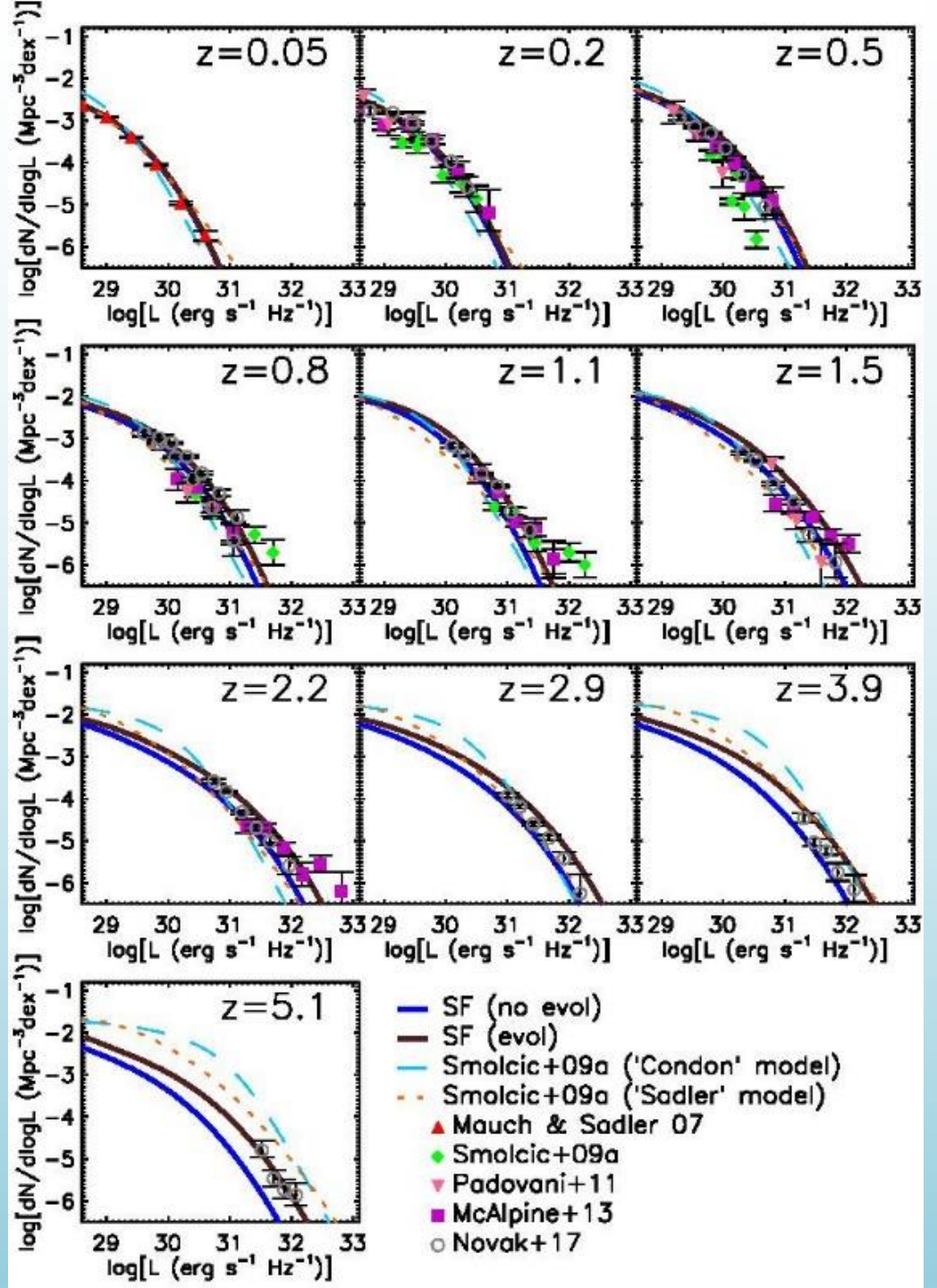

Stronger support to the case for an increase with z of the L_{synch}/SFR ratio is provided by the source counts: without evolution (solid grey line, the counts implied by the L_{synch}–SFR correlation are clearly below the observational determinations while the evolution by Magnelli et al. (2015) leeds to good agreement (solid black line)

The dashed black line illustrates the sensitivity of the counts to the evolution of the L_{synch}/SFR ratio: already with the coefficients of the Magnelli relation at their 1σ limits the evolution yields counts at hundreds of μJy flux densities at the upper limits of observational determinations.

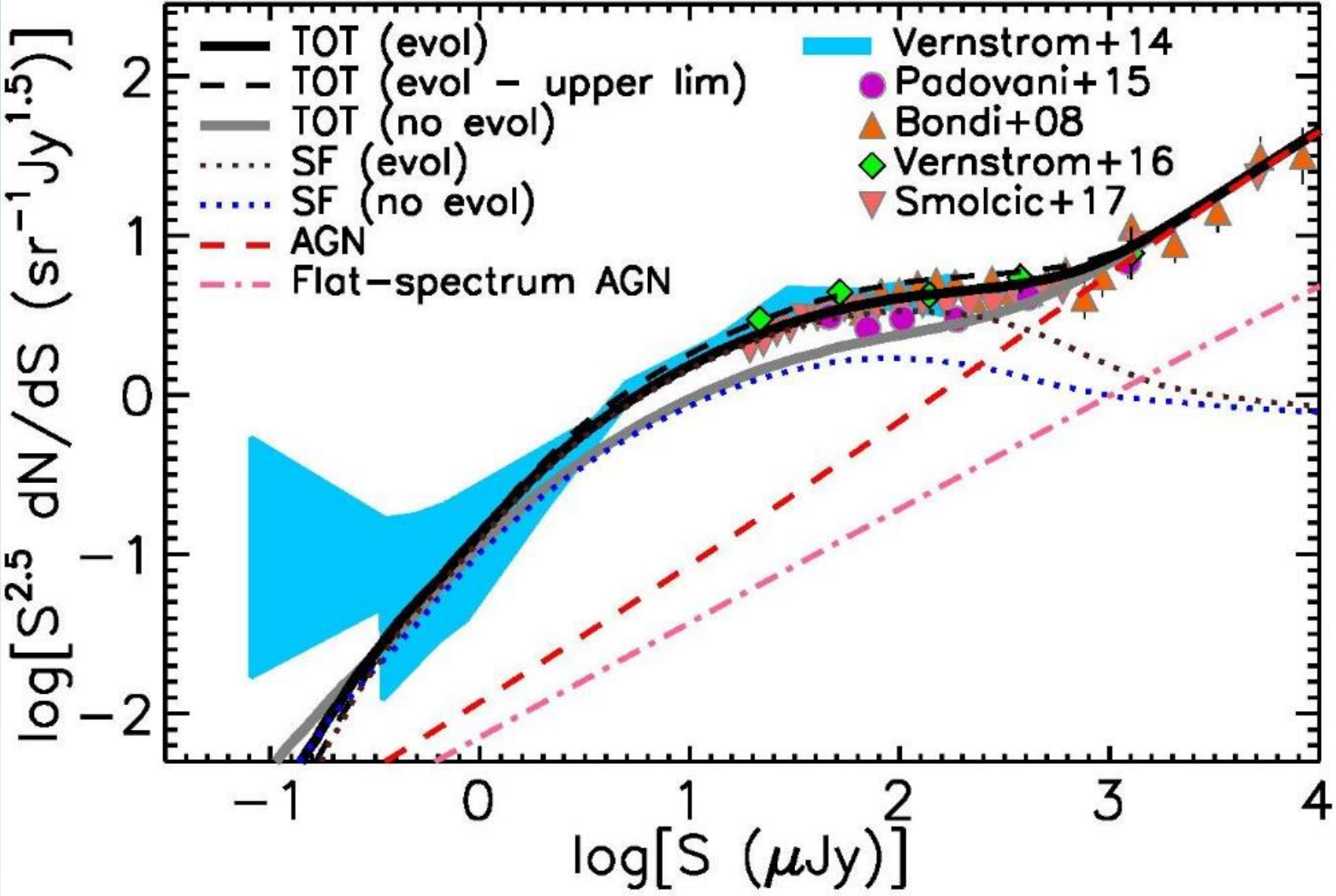

Identification of the faint (sub-mJy) radio-source population -1

- Determining the nature of these sources requires optical/IR spectroscopy to measure the redshift, hence the luminosity, and to classify them as SFGs or AGNs.
- These objects however are very faint in the optical. For example, the median $R_{\rm mag}$ for the Extended C*handra Deep Field*-South (E-CDFS) VLA sample, which reaches $S_{1.4\rm GHz} \sim 32.5$ μJy, is ~ 23; and this refers only to sources detected in the *R* band, while ~ 20% of the objects have only an IR counterpart (Bonzini et al., 2012). Getting spectra for such faint sources is very time consuming (prohibitively so for the very faint tail) but can in principle be done.
- Even if we had optical spectra for all the E-CDFS sources, for faint counterparts one can only see a couple of lines. This is enough to get a redshift but not to properly classify the objects (Padovani 2016).
- The classification thus turns out to be quite complex and has to resort to indicators of varying effectiveness and reliability.

Values of $q_{24obs} = \log(S_{24\mu m}/S_{1.4GHz})$ as a function of redshift for RL AGNs (red squares), RQ AGNs (blue circles) and SFGs (green crosses). The down-pointing arrows represent 3σ upper limits. The solid line shows the evolution of q_{24obs} for the M82 template as a function of redshift with ±2σ dispersion (dashed lines).

The use of the observed flux densities rather than the rest-frame ones minimizes the uncertainties due to the modelling. The continuity of the distribution of q_{24obs} does not allow an unambiguous separation of SFGs from RL AGNs and makes necessary a somewhat arbitrary choice of a SED template.

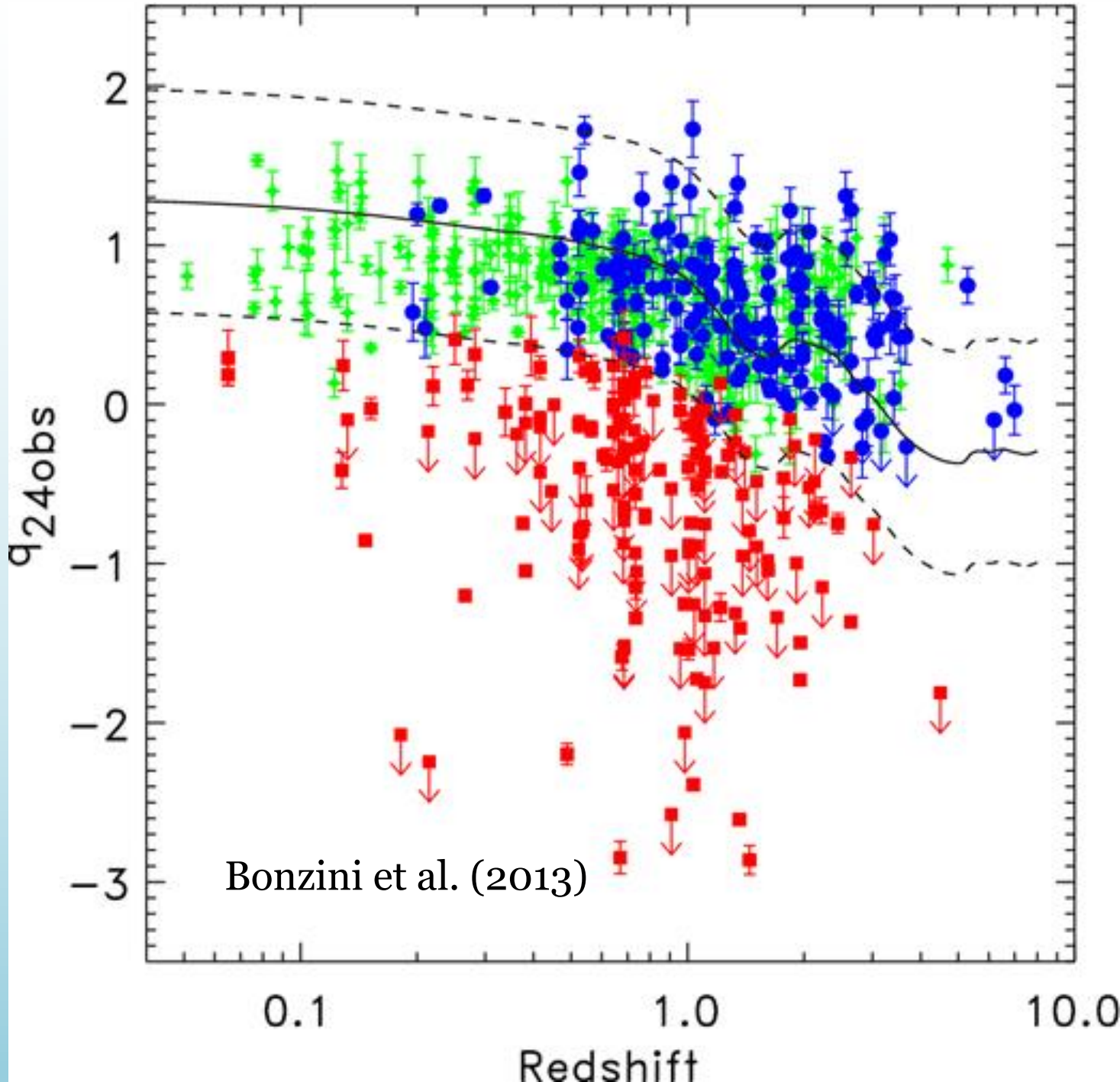

Separation of RQ AGNs from SFGs

- Once RL AGNs have been separated, the remaining faint radio sources can be SFGs or RQ AGNs or a combination of both.
- Direct evidence of an AGN is provided by optical spectra, either through the presence of broad or high-excitation emission lines or via diagnostics based on line ratios. However, most sub-mJy radio sources are too faint in the optical even to determine a redshift. For example, Padovani et al. (2015) could get a spectroscopic redshift for only ~ 40% of the sources.
- The most effective tool to select sources associated to nuclear activity are X-ray observations. SFGs can hardly have ``hard'' X-ray power (2 – 10 keV) $L_x > 10^{42}$ erg s^{-1} (see Szokoly et al., 2004, and references therein). Thus object with $L_x > 10^{42}$ erg s^{-1} are almost certainly AGNs. This however does not mean that there are no AGN below this luminosity.
- Sufficiently deep X-ray observations are however available only over very small areas, such as the central part of the E-CDFS field, covered by the 4 Ms Chandra observations. In this case only the most absorbed AGNs are missed. But in the outer part of the E-CDFS, there are only 250 ks Chandra observations which may not be sensitive even to moderate-luminosity ($10^{42} < L_x < 10^{44}$ erg s^{-1}) AGNs (Bonzini et al. 2013).

IRAC colour - colour diagram

- Whenever X-ray data are missing, the identification of RQ AGNs can be made using deep observations with the *Spitzer* Infrared Array Camera (IRAC) at 3.6, 4.5, 5.8 and 8 μm.
- Different extragalactic sources occupy somewhat different regions in the diagram of the $S_{8.0}/S_{4.5}$ versus $S_{5.8}/S_{3.6}$ ratios (Donley et al., 2012, and references therein). The emission of RQ and RL AGNs can heat up the surrounding dust that re-emits this energy in the mid-IR. If the AGN is sufficiently luminous compared to its host galaxy, the emission from the heated dust can produce a power-law thermal continuum across the four IRAC bands. Sources with this spectral shape occupy a specific region in the IRAC colour–colour diagram, the so-called Lacy wedge (Lacy et al. 2004).
- The completeness of this selection method is therefore high (~ 75%) at $L_x \geq 10^{44}$ erg s^{-1} but relatively low ($\leq$ 20%) for $L_x \leq 10^{43}$ erg s^{-1}. IRAC selection appears also to be incomplete to radio galaxies (Donley et al. 2012).
- Nevertheless, mid-IR (MIR) selection is very important since it identifies also heavily obscured AGN (provided that they are not hosted by a particularly bright galaxy), many of which are missed even by deep X-ray surveys (Donley et al., 2012).

IRAC colour plot for RL AGNs (red squares), RQ AGNs (blue circles) and SFGs (green crosses). The black cross on the top left shows the typical uncertainties.

The black line encloses the ‘Donley wedge’ (Donley et al. 2012), sources whose AGN emission dominates the MIR populate this region.

Colour–colour tracks of a 13 Gyr old elliptical galaxy (long dashed line), a spiral galaxy (dot–dashed line), a type 2 Seyfert galaxy (dashed line) and a type 1 QSO (dotted line) (Polletta et al. 2007) in the redshift range 0.1–3 are also plotted.

As shown by their colour–colour track, Type 2 Seyfert galaxies are easily missed by this diagram.

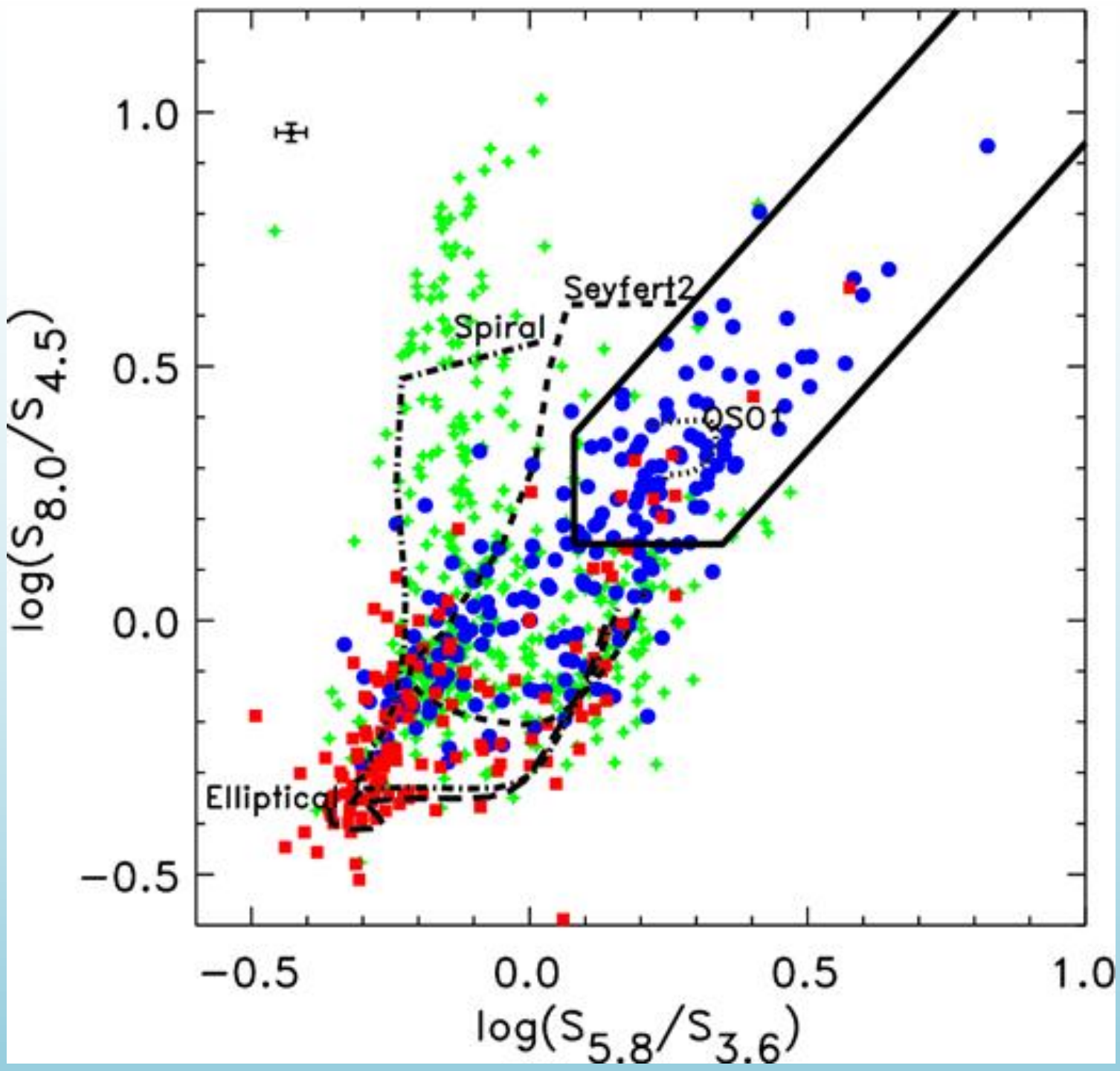

Source classification: summary

In short, to classify faint radio sources:

- one first selects RL AGN using a variant of the IR – radio correlation;
- then separates the RQ AGN from SFGs using L_X;
- next, the IRAC colour-colour diagram is used to recover (RQ) AGN missed by the X-ray criterion;
- Finally, other indicators (radio spectra, radio morphology, optical lines, optical photometry, …), if available are applied to catch possible outliers.

The classification work has demonstrated that early work overestimated the fraction of SFGs among sub-mJy sources. This was caused by a selection effect: SFGs have higher optical to radio luminosity ratios than RL AGNs and therefore are over-represented in samples identified through magnitude limited optical imaging. Only ~ 44% of the complete sample of sub-mm radio sources studied by Windhorst et al. (1985) were optically identified, and ~70% of these were found to be galaxies, mostly blue (star forming). But this fact did not warrant that the majority of sub-mJy sources are star-forming galaxies, as assumed by several authors.

The figure shows one of the most accurate current estimates of the fractions of the various classes of radio sources as a function of the flux density at 1.4 GHz: SFGs (green diamonds) , all AGNs (black triangles), RQ AGNs (blue circles) and RL AGNs (red squares). RL AGNs go from being totally dominant at ≥ 1 mJy to being ~ 10% at the survey limit. SFGs, become dominant below 0.1 mJy, reaching ~ 60% at the survey limit. The fraction of RQ AGNs increases at lower flux densities; they make up 75% of all AGN and ≈ 29% of all sources at the survey limit, up from ≈ 6% at ≈ 1 mJy.

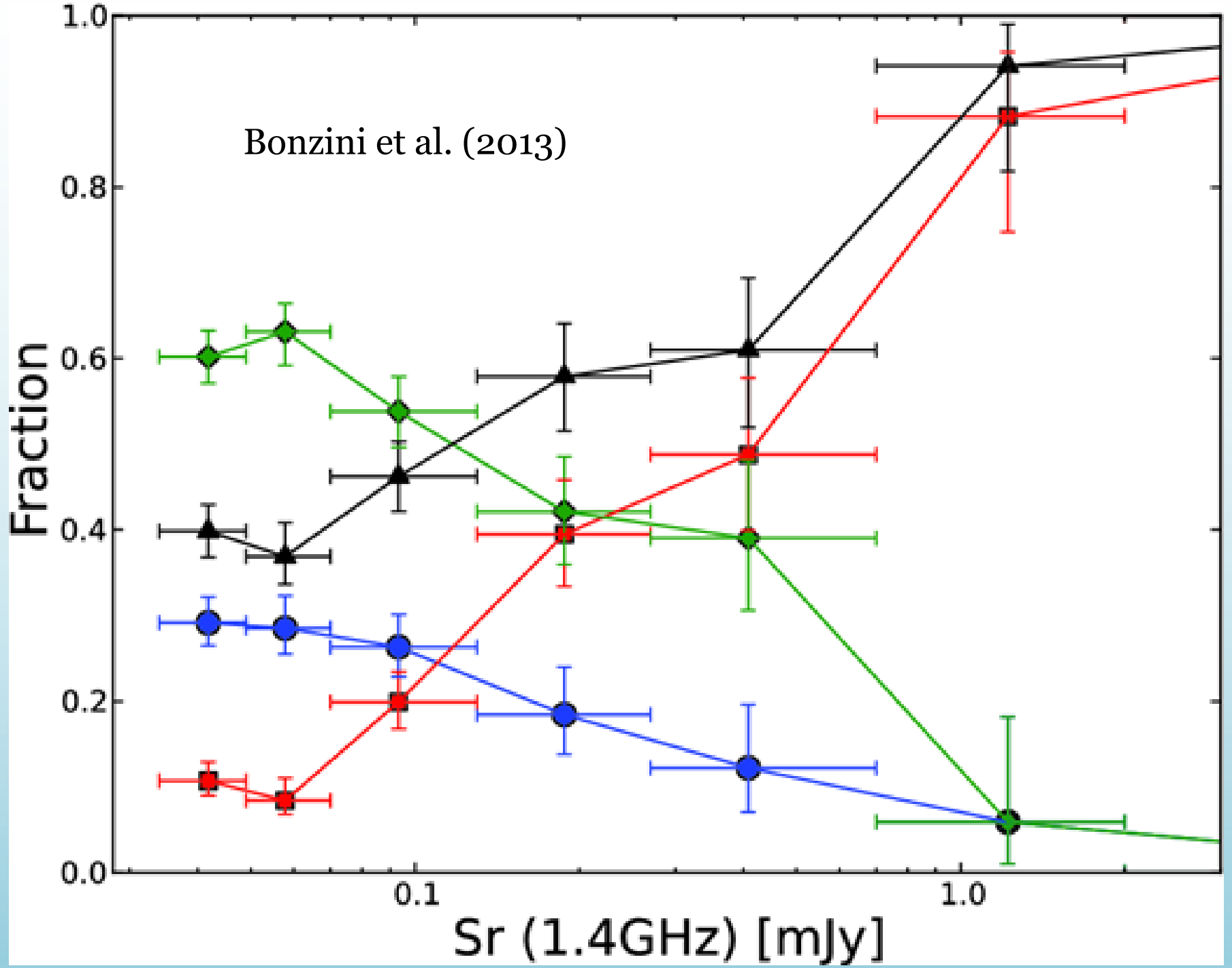

Radio quiet (RQ) AGNs: a new radio source population? - 1

- Soon after the discovery of the first quasar, a very strong radio source ($S_{1.4\ \mathrm{GHz}} \sim 50$ Jy), it was realised that there were many more similar sources, which were undetected by the radio telescopes of the time: they were “radio-quiet” (Sandage, 1965).
- These sources, which make up the majority (> 90%) of the AGN class were later understood to be perhaps only “radio-faint”, as for the same optical power their radio powers were ≈ 3 orders of magnitude smaller than their radio-loud (RL) counterparts.
- As we have seen, identifications of sub-mJy radio sources have revealed the presence of a substantial fraction RQ AGNs associated to faint objects (Padovani et al. 2009, Bonzini et al. 2013). Evidence of nuclear activity in these sources comes from one or more bands of the electromagnetic spectrum (e.g. optical, mid-infrared, X-ray) but the origin of their radio emission is still being hotly debated.
- High resolution radio observations have provided evidence that some RQ AGNs have components with very high surface brightness, variability, or apparent super-luminal motion, all of which are characteristic of emission driven by a super massive BH (Herrera Ruiz et al. 2016, Maini et al. 2016).
- White at al. (2017) have found that, for the majority of RQQs in their z ~1 sample, the dominant source of radio emission is connected to the AGN rather than star formation in the host galaxy.

Radio quiet (RQ) AGNs: a new radio source population? - 2

However this does not necessarily prove that the general RQ AGN population possesses radio cores that contribute substantially to the total radio emission.

- Based on their study of the E-CDFS VLA sample Padovani et al. (2015) concluded that RQ and RL QSOs are two totally distinct AGN populations, characterized by very different evolutions, luminosity functions, and Eddington ratios. The radio power of RQ AGNs evolves similarly to SFGs, consistent with their radio emission being powered by star formation.
- This conclusion was confirmed by the study of Bonzini et al. (2015) who used deep *Herschel* photometry to determine the FIR emission, hence the SFR, of E-CDFS galaxies.
- Further support to this view was provided by Kellermann et al. (2016) who, based on 6 GHz Jansky Very Large Array (JVLA) observations of a volume-limited sample of 178 low redshift optically selected QSOs, argued that the bulk of the radio emission of RQ QSOs is powered by star formation in their host galaxies (see also Kimball et al. 2011, Condon et al. (2013).
- The analysis by Bonato et al. (2017) is fully consistent with the hypothesis that the radio emission associated to star formation can account for the statistical properties (number counts, redshift-dependent luminosity functions) of faint radio sources.

Conclusions at this point

- The faint radio sky plays an important role in a variety of astrophysical topics, including the cosmic star formation history, galaxy evolution, the existence of powerful jets, and radio emission in RQ AGNs.
- The source populations of the sub-mJy GHz radio sky have been sorted out. Below ≈ 0.1 mJy the radio sky is dominated by SFGs. Assessing the composition of sub-mJy sources took more than thirty years because the multi-wavelength data necessary to properly classify sources were not available and radio astronomy was ahead of the other bands.
- The role of radio astronomy for a whole range of extragalactic studies related to star formation and galaxy and AGN evolution will grow in the near future. Radio observations are unaffected by absorption, which means, for example, that they can dig out the most extremely dust-enshrouded star-forming regions and are sensitive to all types of AGN, irrespective of obscuration and orientation (i.e., Type 1s and Type 2s).
- Radio astronomy is at the verge of a revolution thanks to the Square Kilometre Array (SKA) that will reach flux limits orders of magnitude fainter than it is currently possible, and over large areas.
- But the full exploitation of the SKA potential requires synergies with other multi-wavelength astronomical such as *Athena*, WFIRST, the LSST, the ELTs, JWST, and SPICA.

Square Kilometre Array

3 sites; 2 telescopes + HQ

Design Phase: > €170M; 600 scientists+engineers

Phase 1

Construction: 2018 – 2024

Construction cost cap: €674.1M (inflation-adjusted)

Operations cost: under development

Phase 2: start mid-2020s

~2000 dishes across 3500 km of Southern Africa

Major expansion of SKA1-Low across Western Australia

Diamond, *SKA Director-General*
SKA Community briefing 18 Jan 2017

What is the SKA?

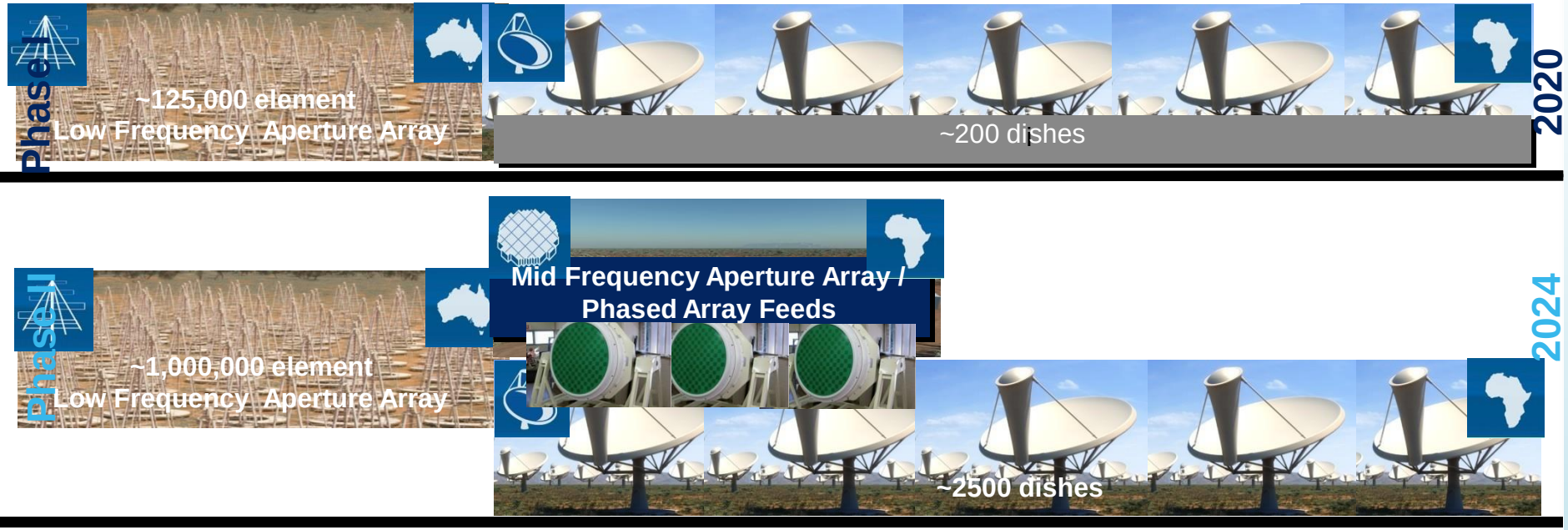

SKA Organisation: 10 countries, more to join

Australia (DoI&S)
Canada (NRC-HIA)
China (MOST)
India (DAE)
Italy (INAF)
Netherlands (NWO)
New Zealand (MED)
South Africa (DST)
Sweden (Chalmers)
UK (STFC)

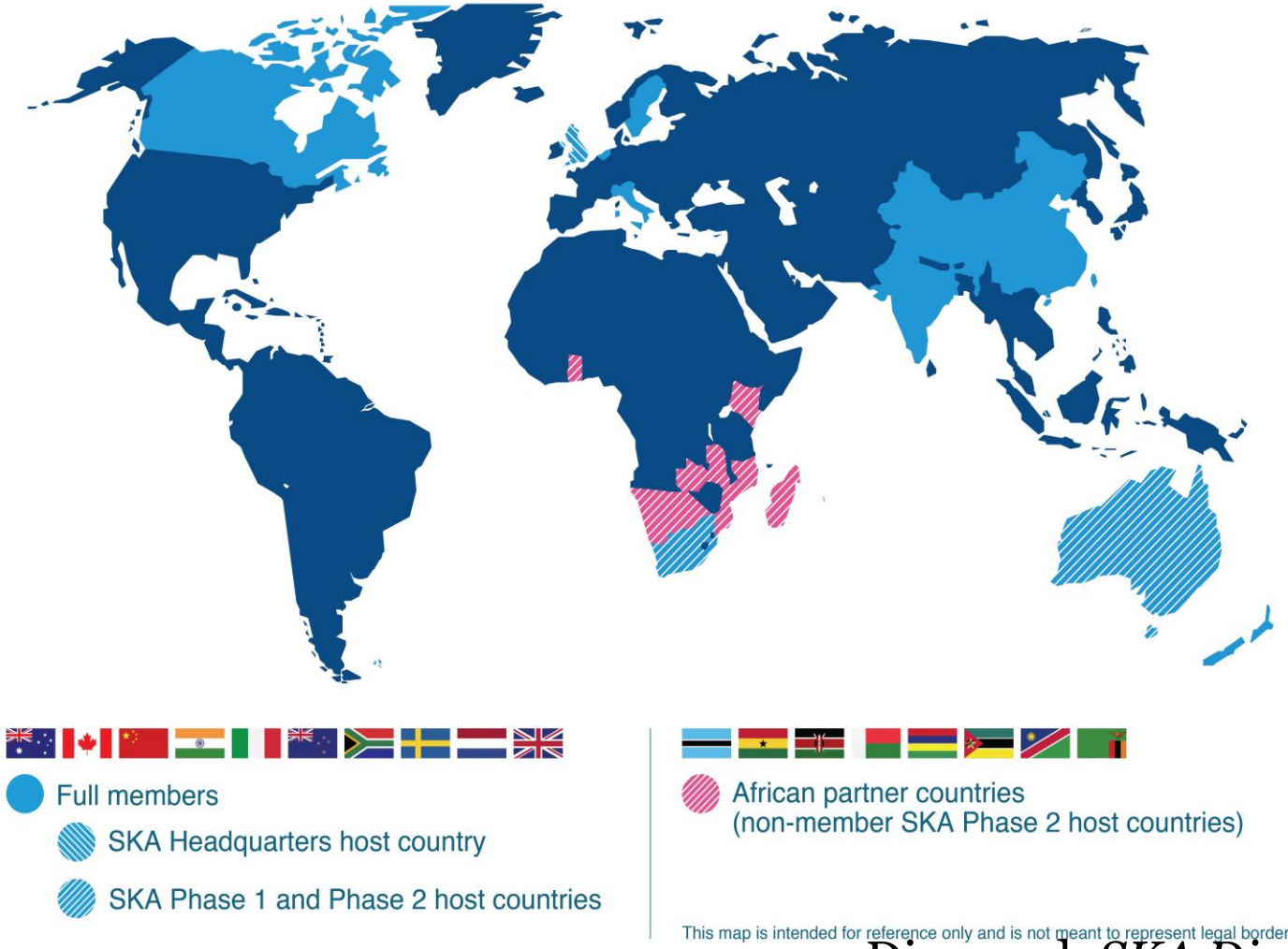

Interested Countries:

- France
- Germany
- Japan
- Korea
- Malta
- Portugal
- Spain
- Switzerland
- USA

Contacts:

- Mexico
- Brazil
- Ireland
- Russia

Diamond, *SKA Director-General*
SKA Community briefing 18 Jan 2017

SKA: HQ in UK; telescopes in AUS & RSA

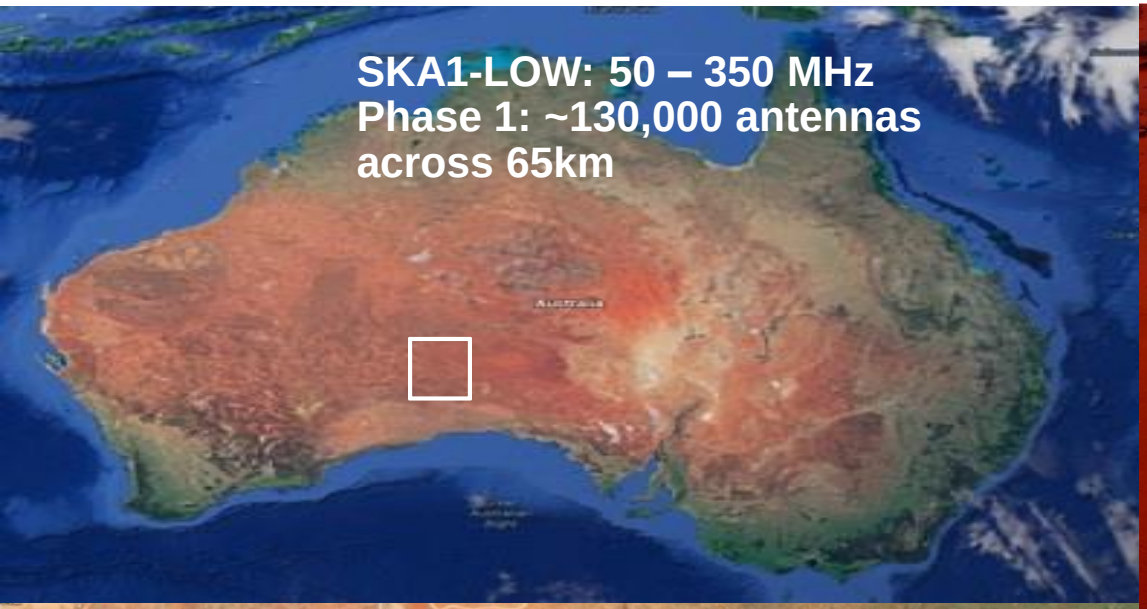

Construction: 2018 – 2024; Cost cap: €675M

Terrestrial Interference

Forte satellite: 131MHz

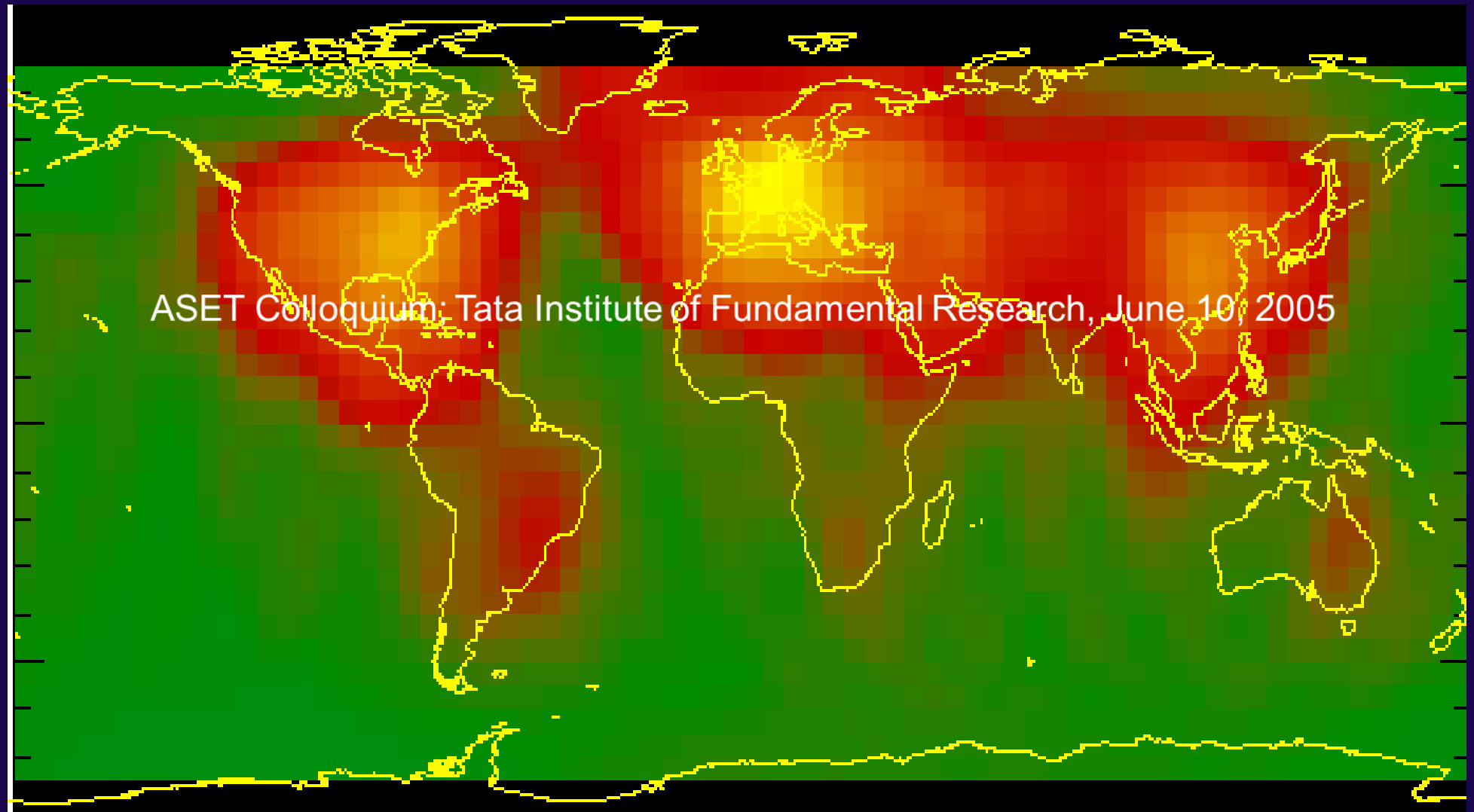

SKA1 Configurations

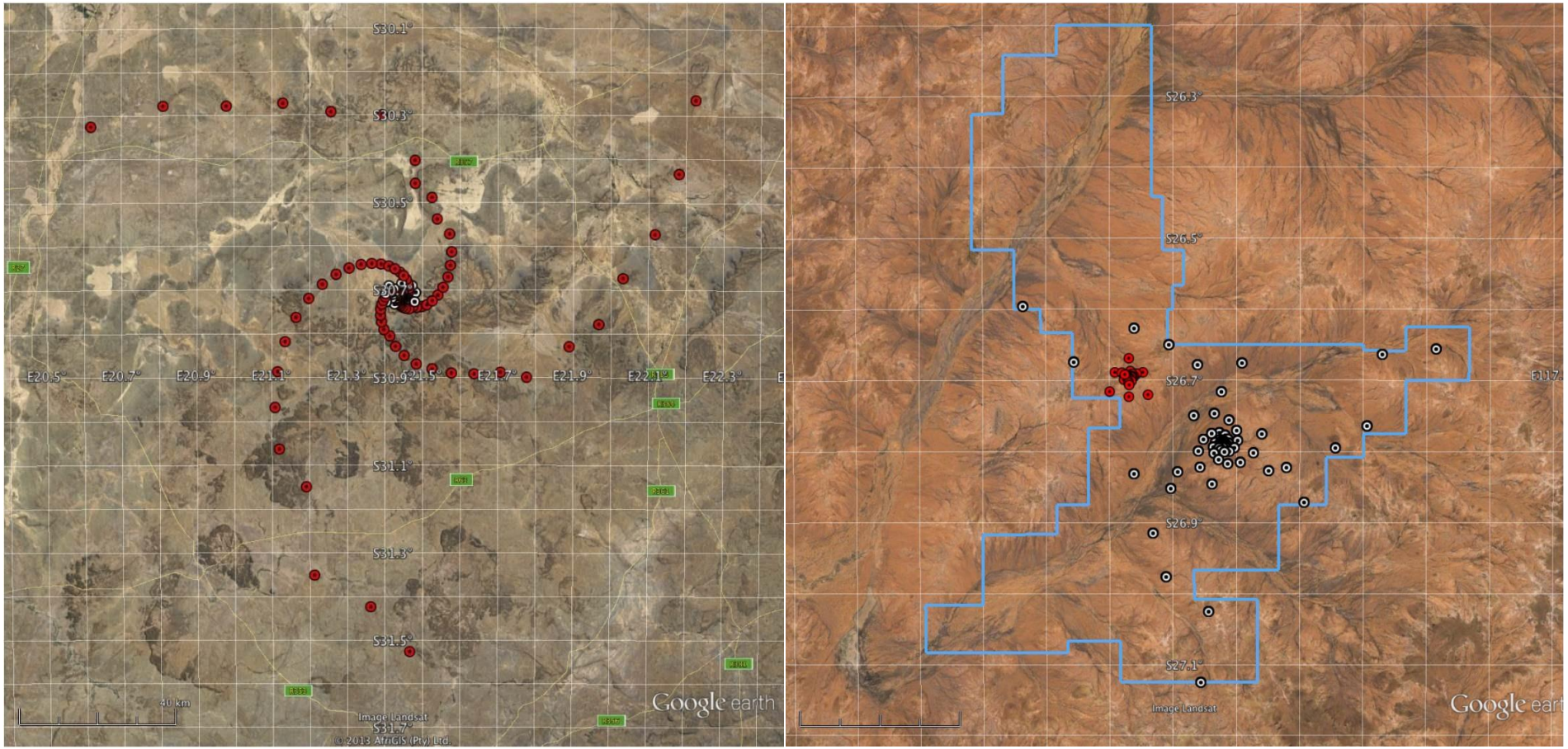

- SKA1–MID, –LOW: B_{Max} = 156, 65 km

SKA2 Configurations

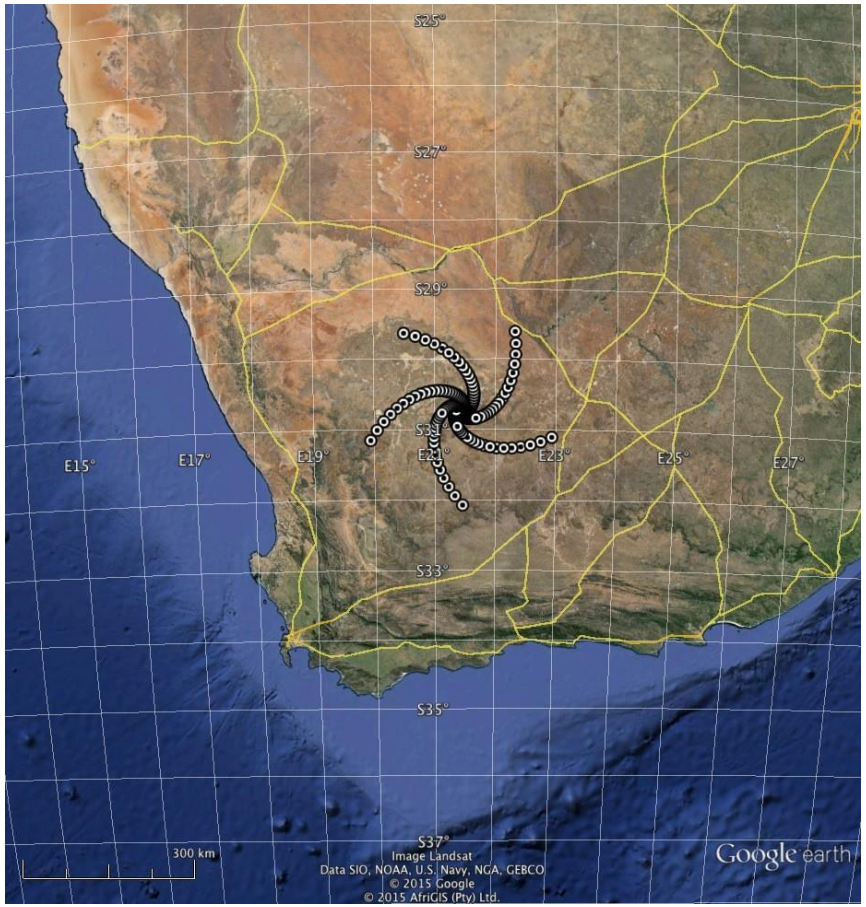

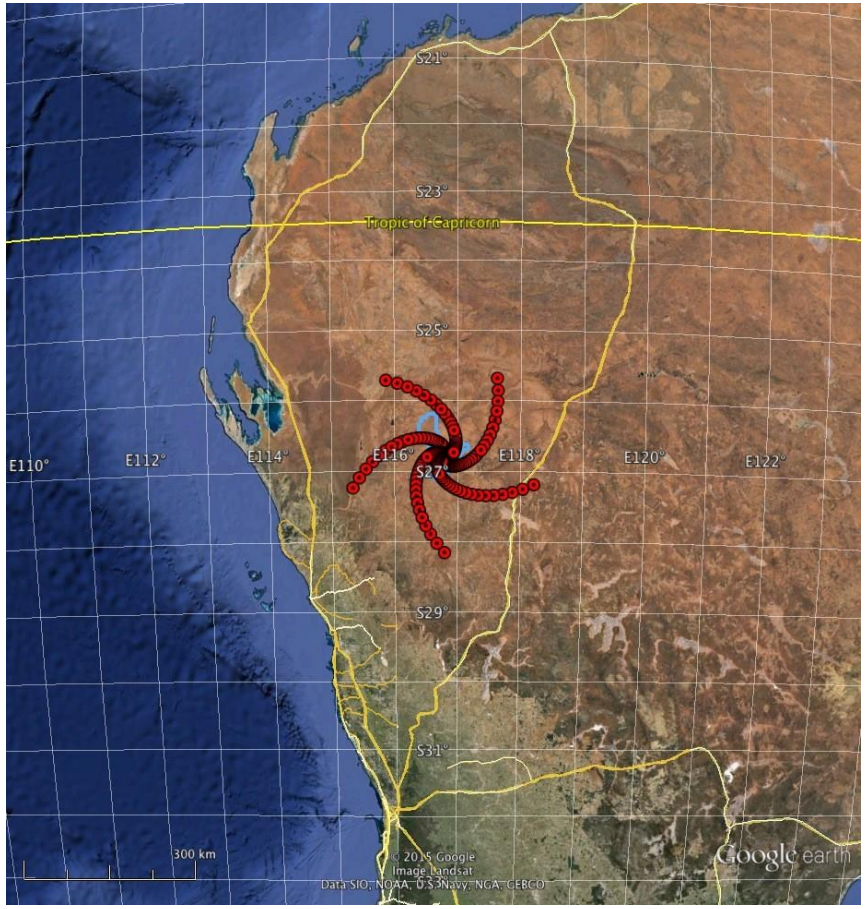

- SKA2–Dish, –LOW: B_{max} ≈ 300 km “core”, ≈3000+ km remote

SKA Science Book 2015

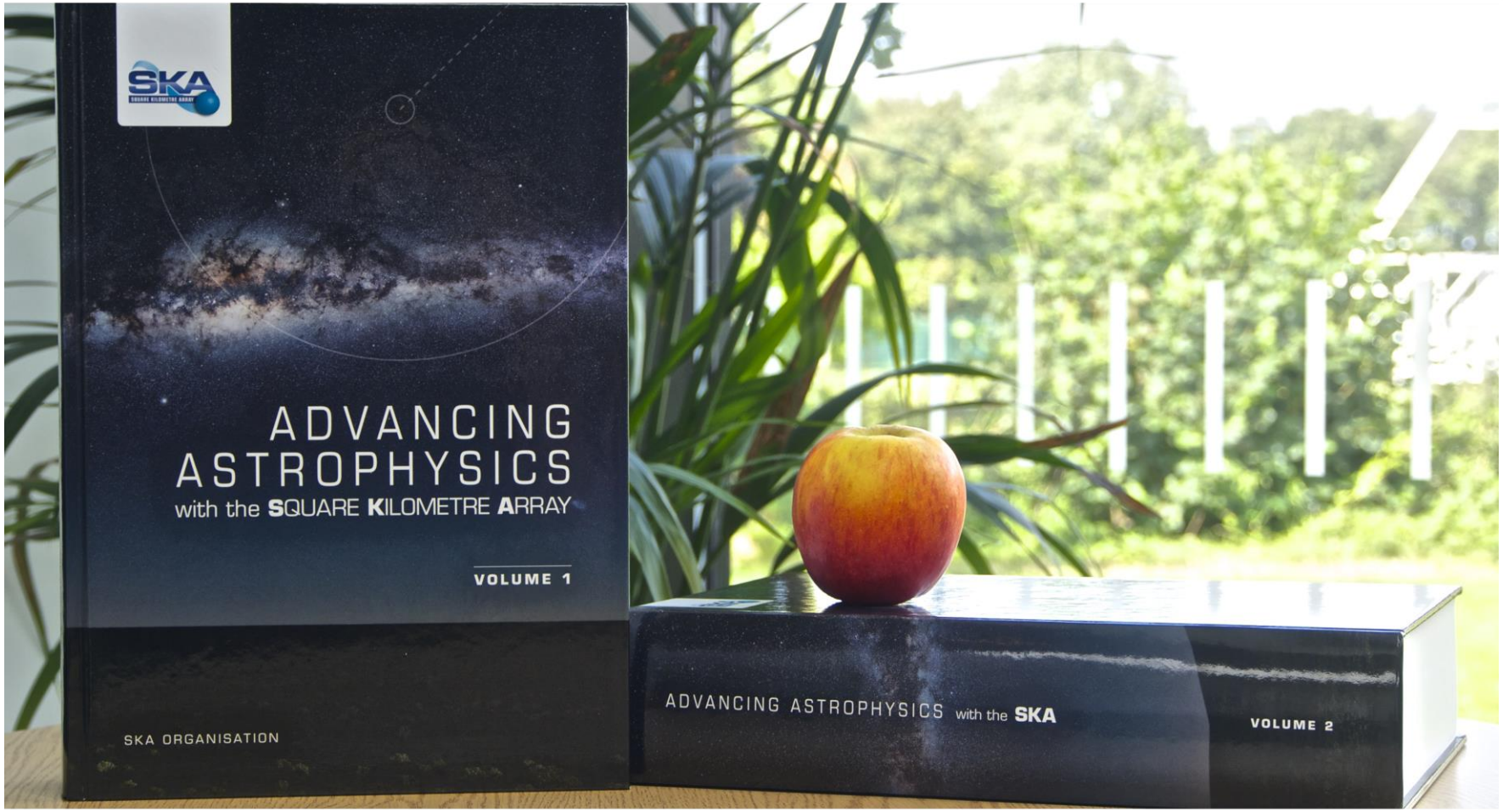

- 135 Chapters, 2000 pages, 8.8 kg
- Plus new science directions that continue to emerge!

Diamond, SKA Director-General
SKA Community briefing 18 Jan 2017

SKA Science Working Groups

- Current SWGs represent a wide range of scientific areas:
  - Extragalactic Spectral Line (non-HI)
  - Our Galaxy
  - Solar, Heliospheric & Ionospheric Physics
  - Epoch of Reionization
  - Cosmology
  - Extragalactic Continuum (galaxies/AGN, galaxy clusters)
  - Cradle of Life
  - HI galaxy science
  - Magnetism
  - Pulsars
  - Transients
- Technique focused Working Group:
  - VLBI
- Topical Focus Group:
  - High Energy Cosmic Particles

Membership open to any active researcher with willingness to contribute at appropriate level

Anyone can nominate themselves by contacting the current SWG Chairperson (per web site) or SKA Project Scientist/Science Director

Diamond, *SKA Director-General*
SKA Community briefing 18 Jan 2017

SKA1-MID

SKA1-LOW

SKA's 1^{o} field-of-view

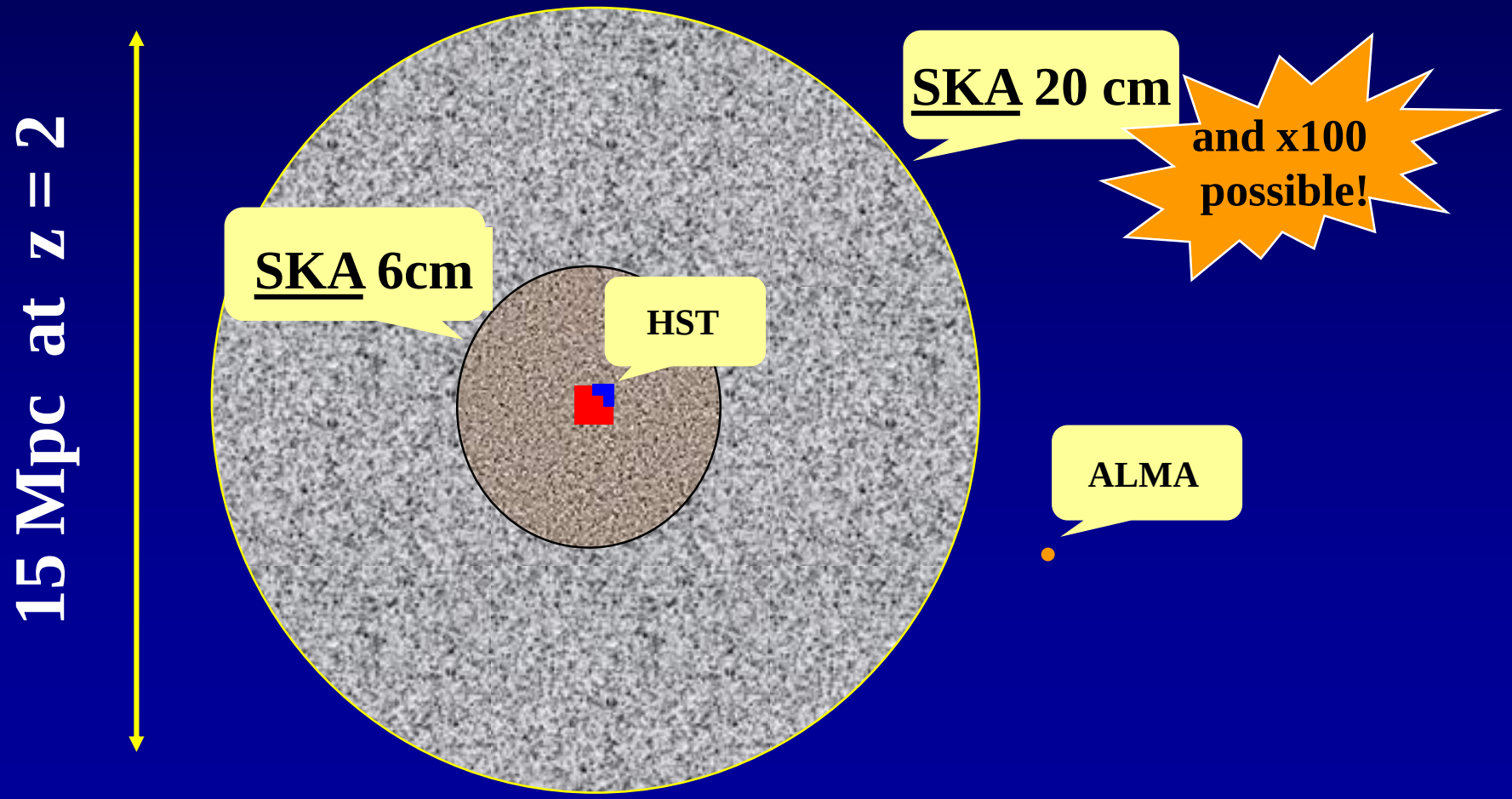

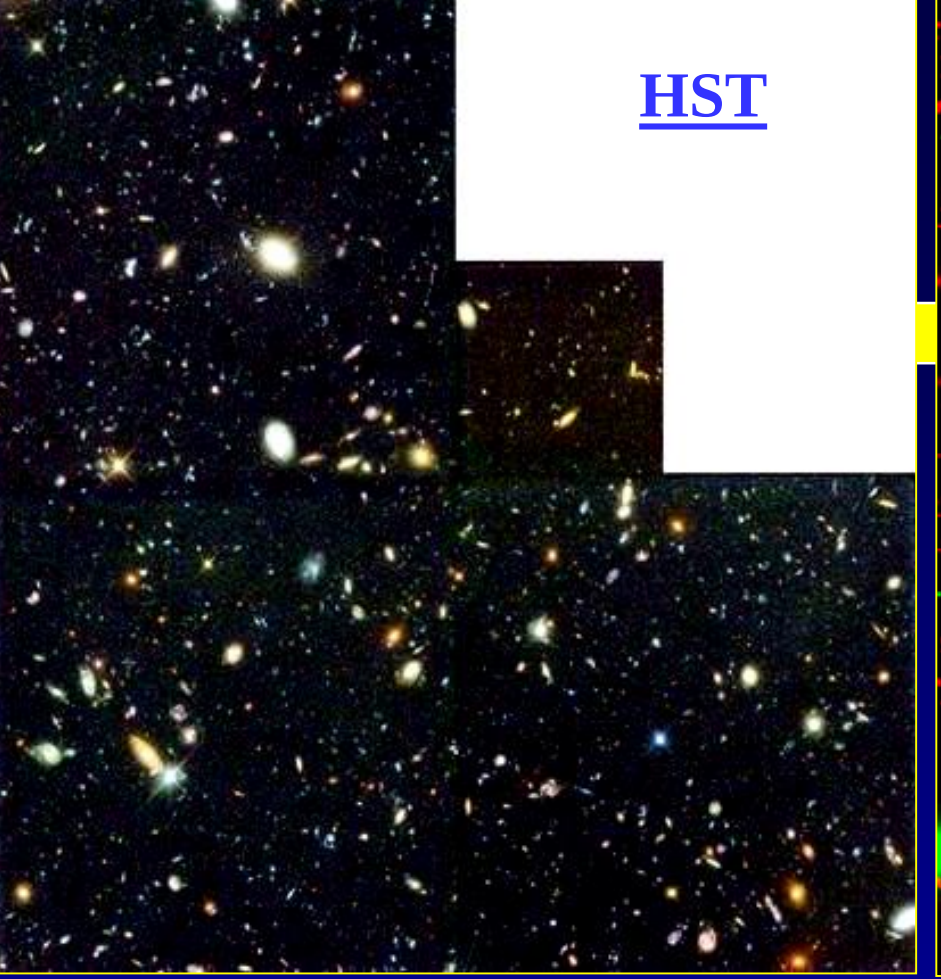

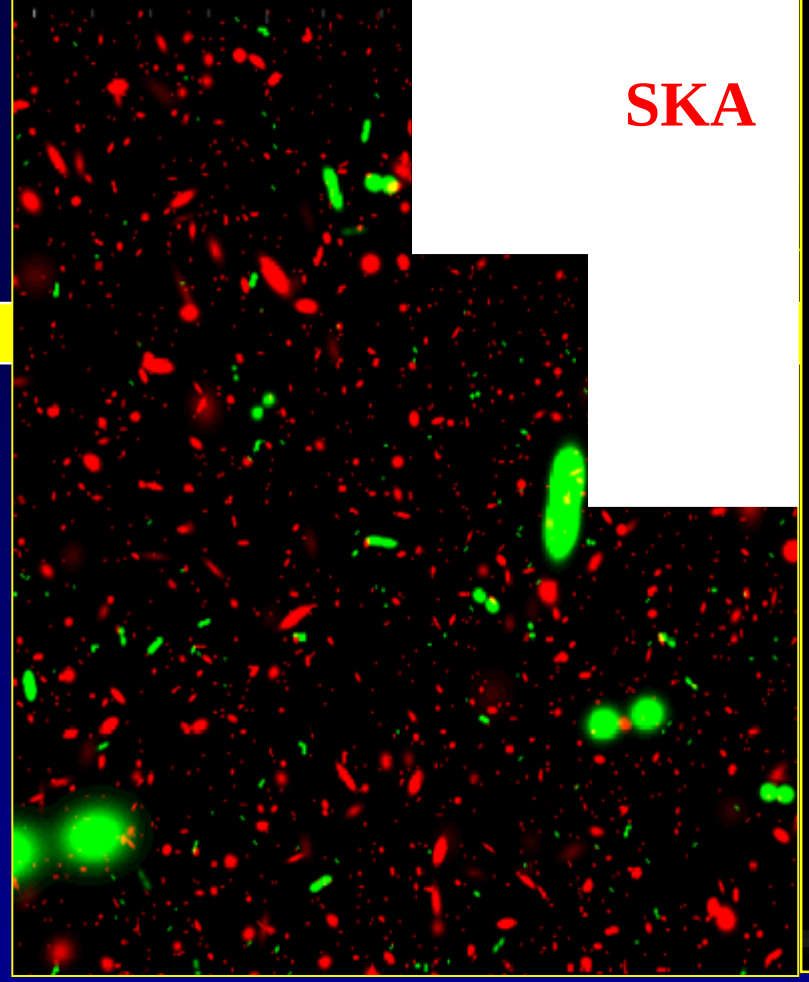

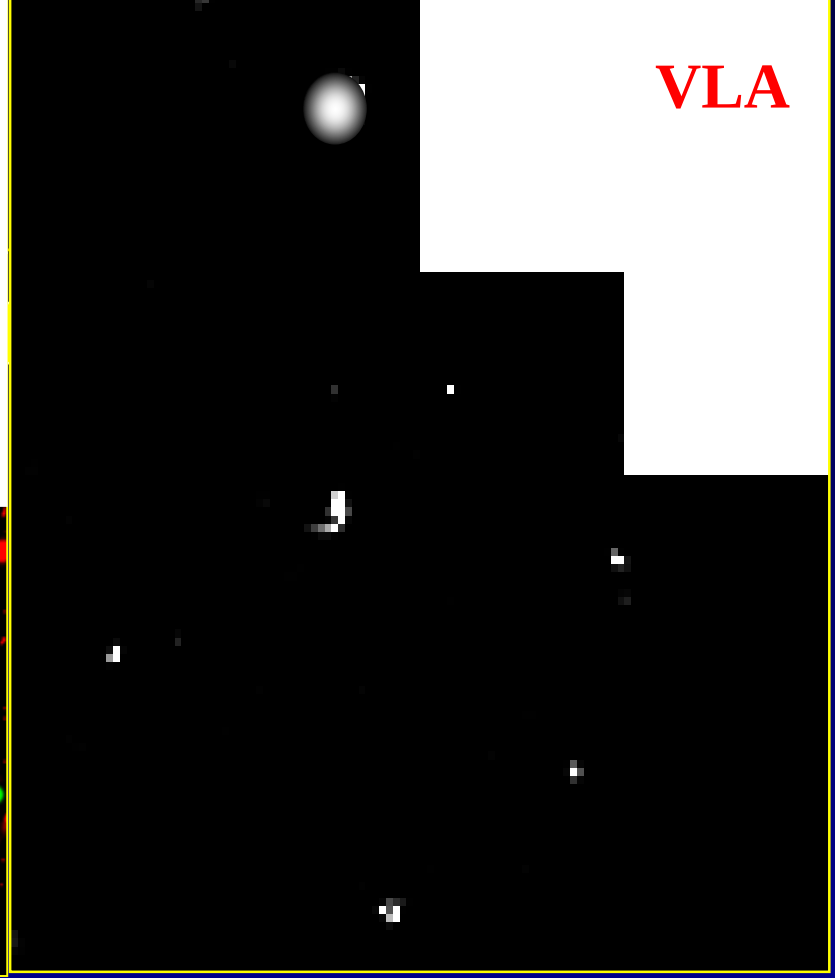

Hubble deep field image compared with the VLA 8.7GHz image of the same area (Fomalont et al. 1997) and with an .SKA simulation for the same area. The VLA image required 50 hours integration and detected 6 sources above 12 μJy. The SKA simulation (Hopkins et al. 2000) assumes 0.1 μJy limit at 1.4GHz and extrapolates using a model based on the LFs for radio, starburst and normal galaxies. The double lobed radio galaxy population are shown as doubles with random orientation, the radio emission from normal and starburst galaxies is shown with galaxy shaped images. At this flux level the field is dominated by normal galaxies; these have comparable densities to the galaxies detected by Hubble. The actual field imaged by the SKA will be very much larger than that shown for the HDF. From R. Ekers, Open Questions in Cosmology, Munich Aug 22-26 2005

Image Quality Comparison

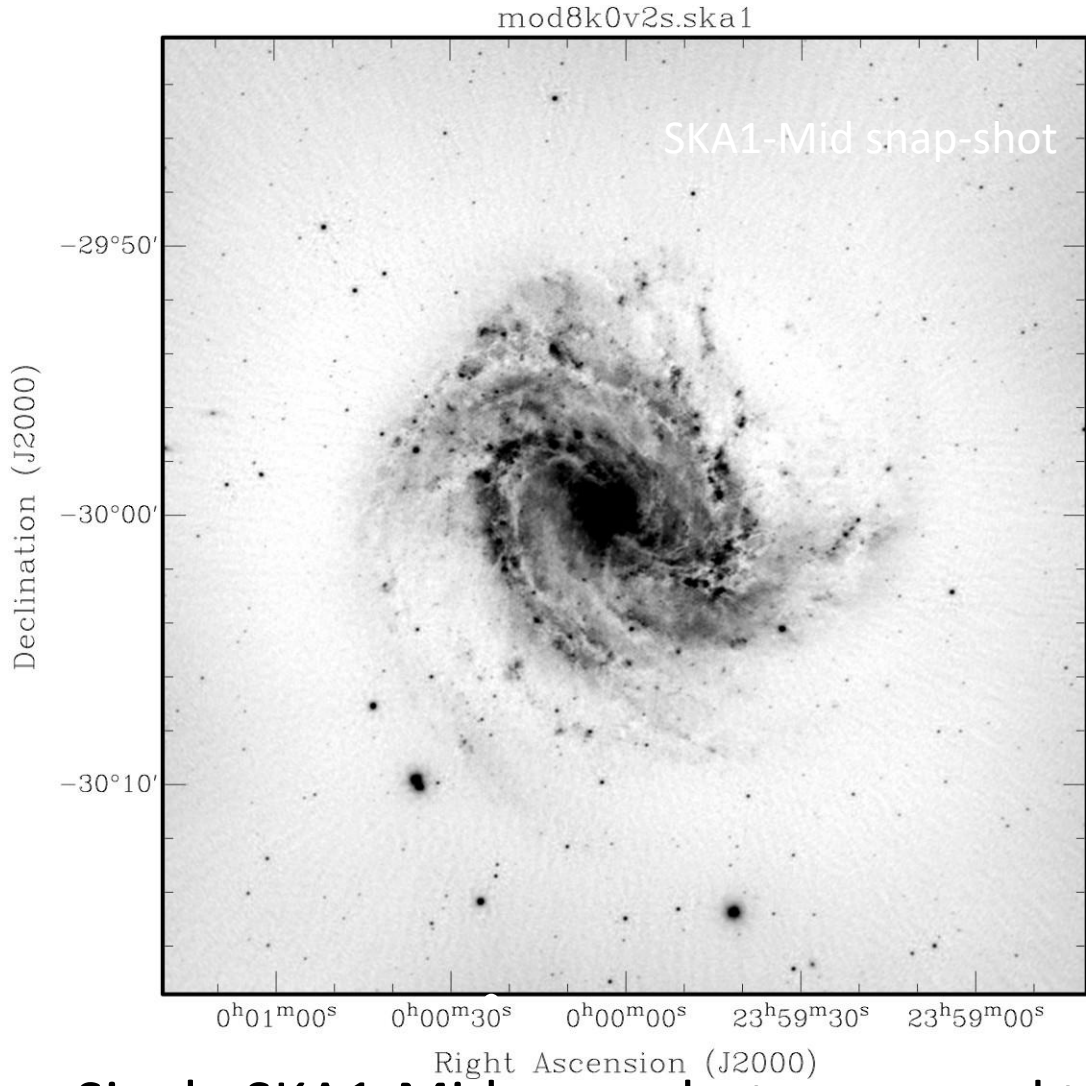

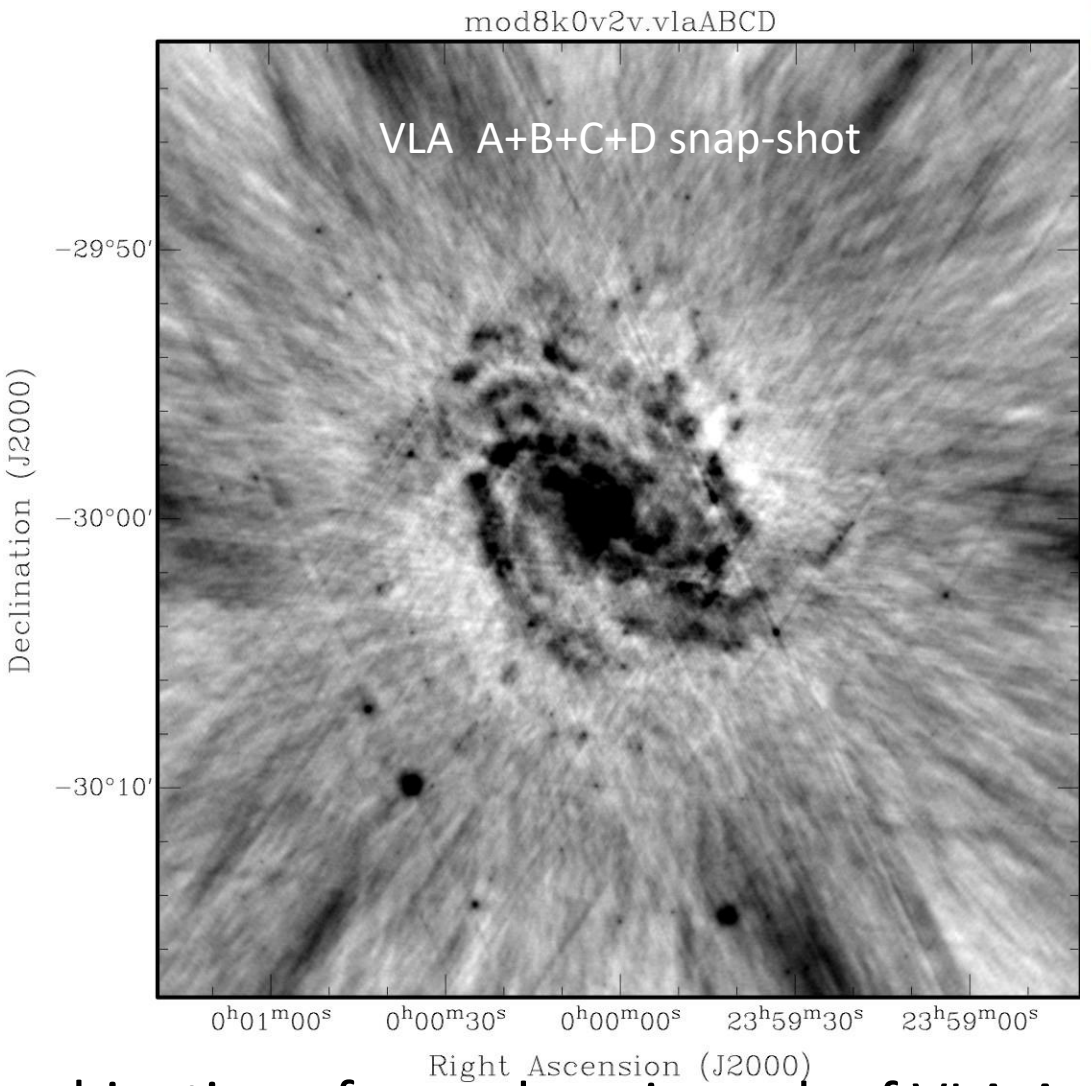

Single SKA1-Mid snap-shot compared to combination of snapshots in each of VLA A+B+C+D.
Diamond, *SKA Director-General* SKA Community briefing 18 Jan 2017

Image Quality Comparison

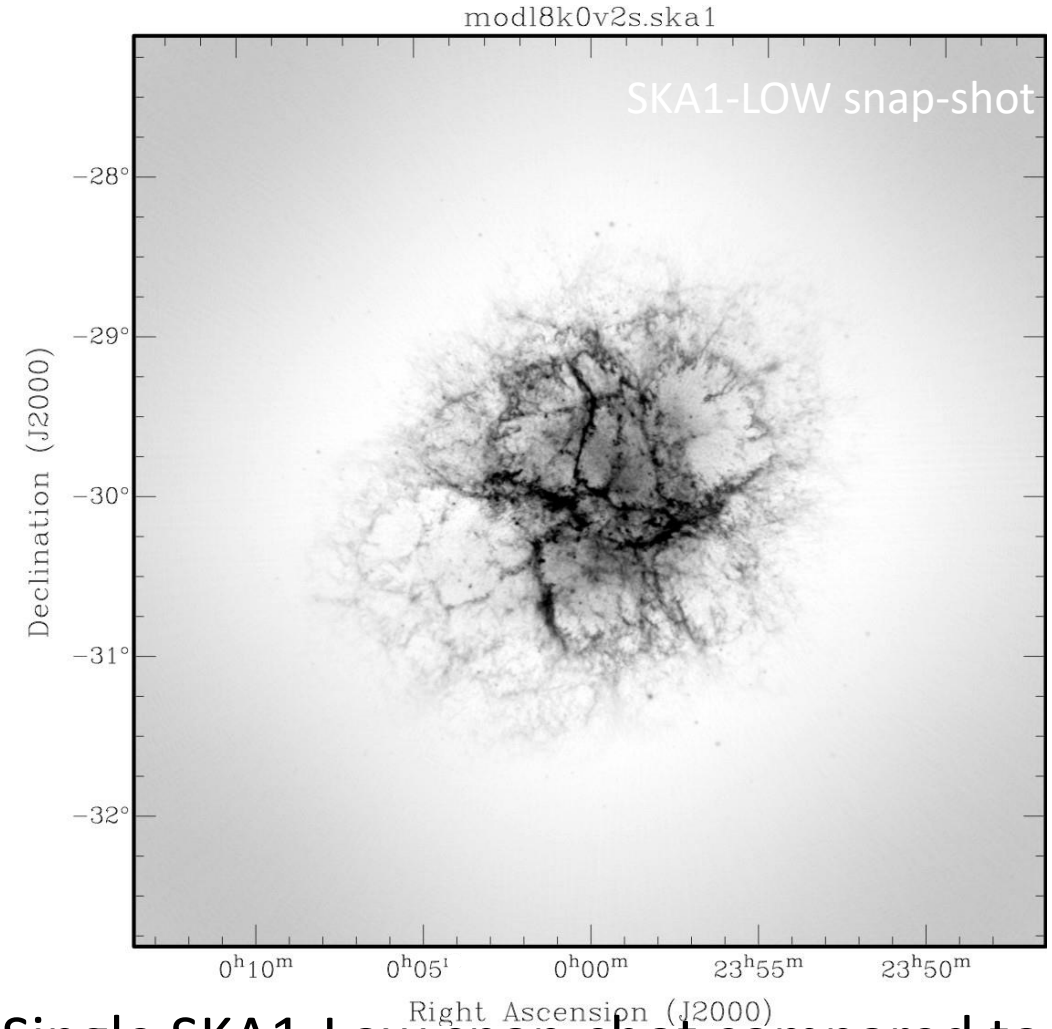

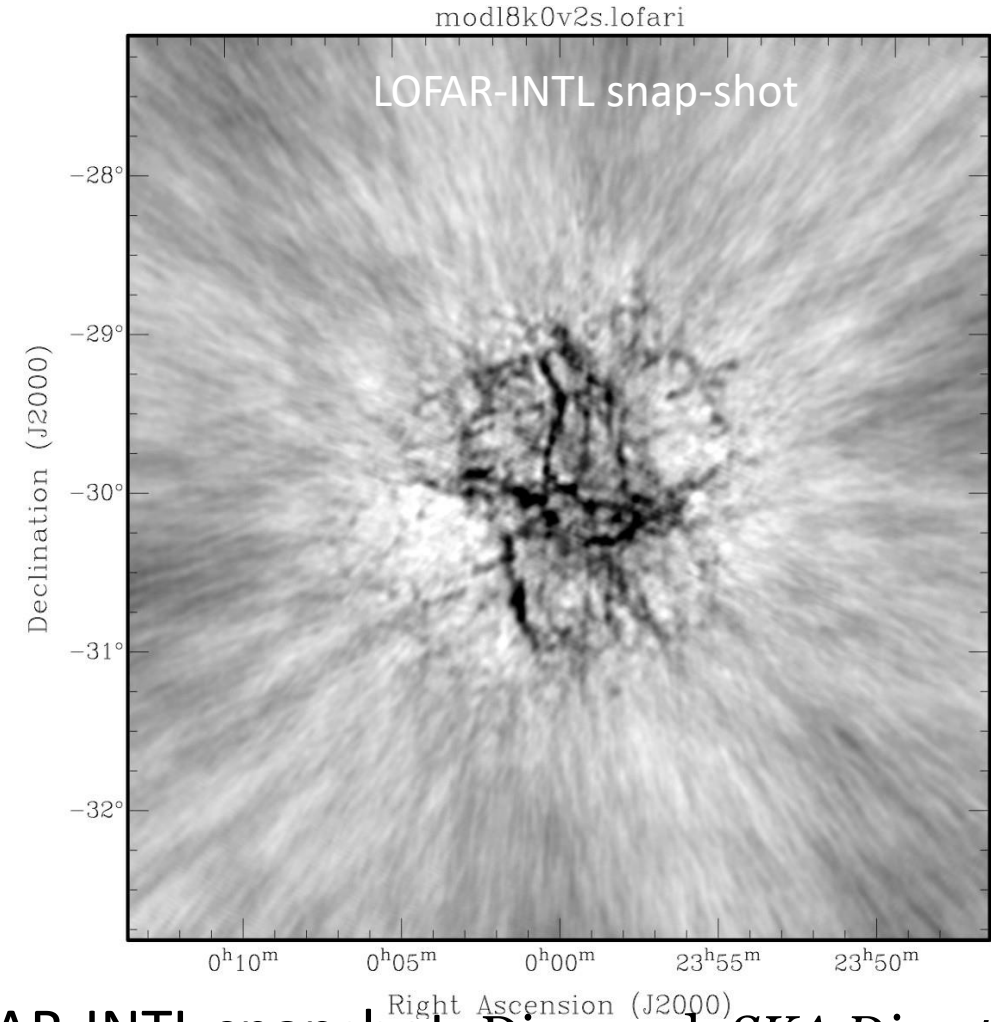

Single SKA1-Low snap-shot compared to LOFAR-INTL snapshot. Diamond, *SKA Director-General* SKA Community briefing 18 Jan 2017.

SKA1 capability vs state-of-the-art

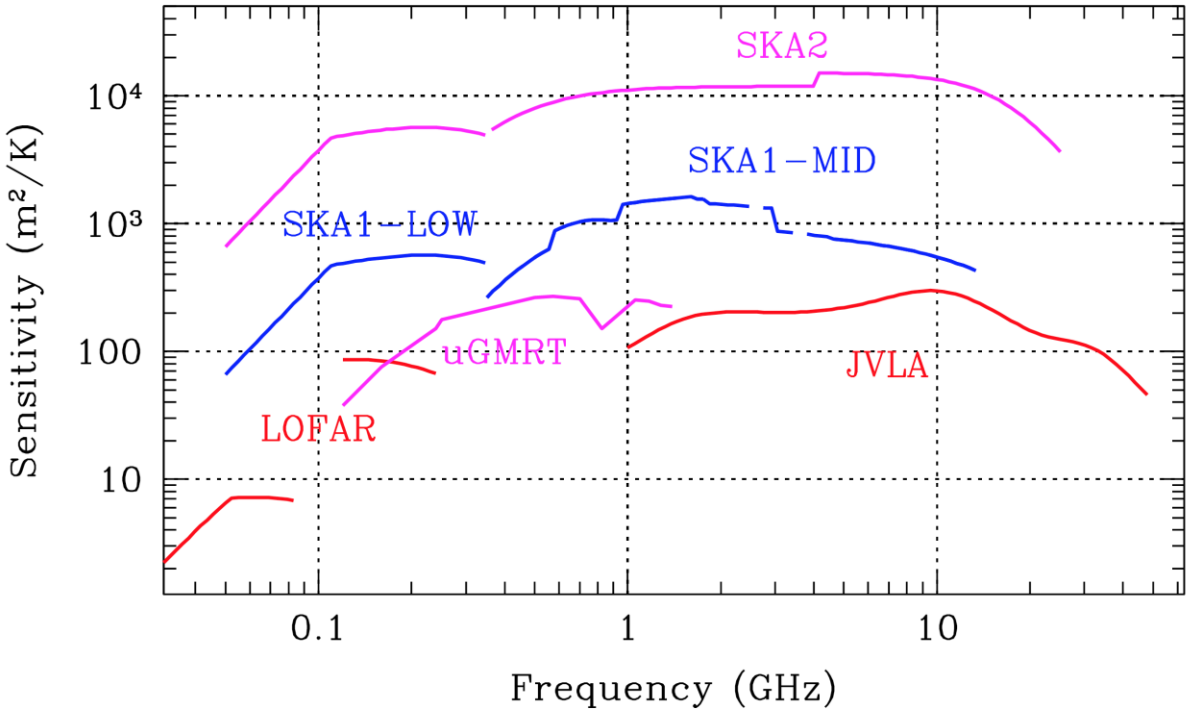

Point-source sensitivity:
~ 4 – 20 times state-of-the-art

Survey speed:
~ 10 - 100 times state-of-the-art

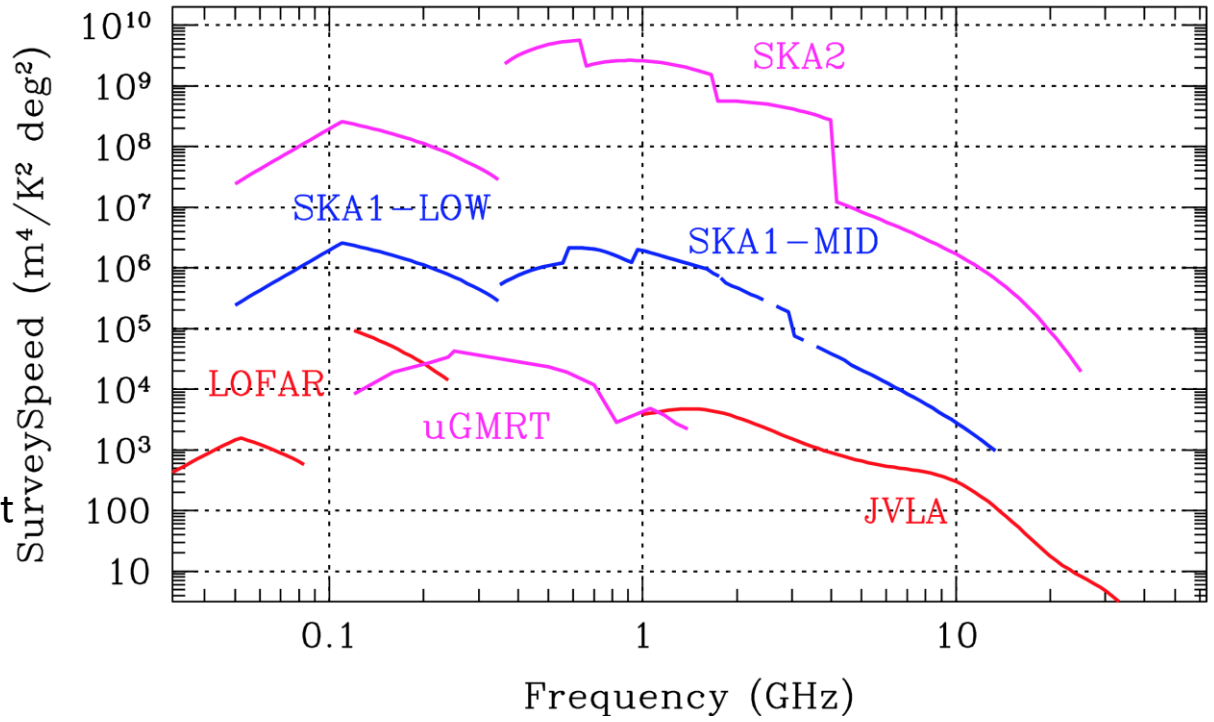

Diamond, *SKA Director-General* SKA Community briefing 18 Jan 2017

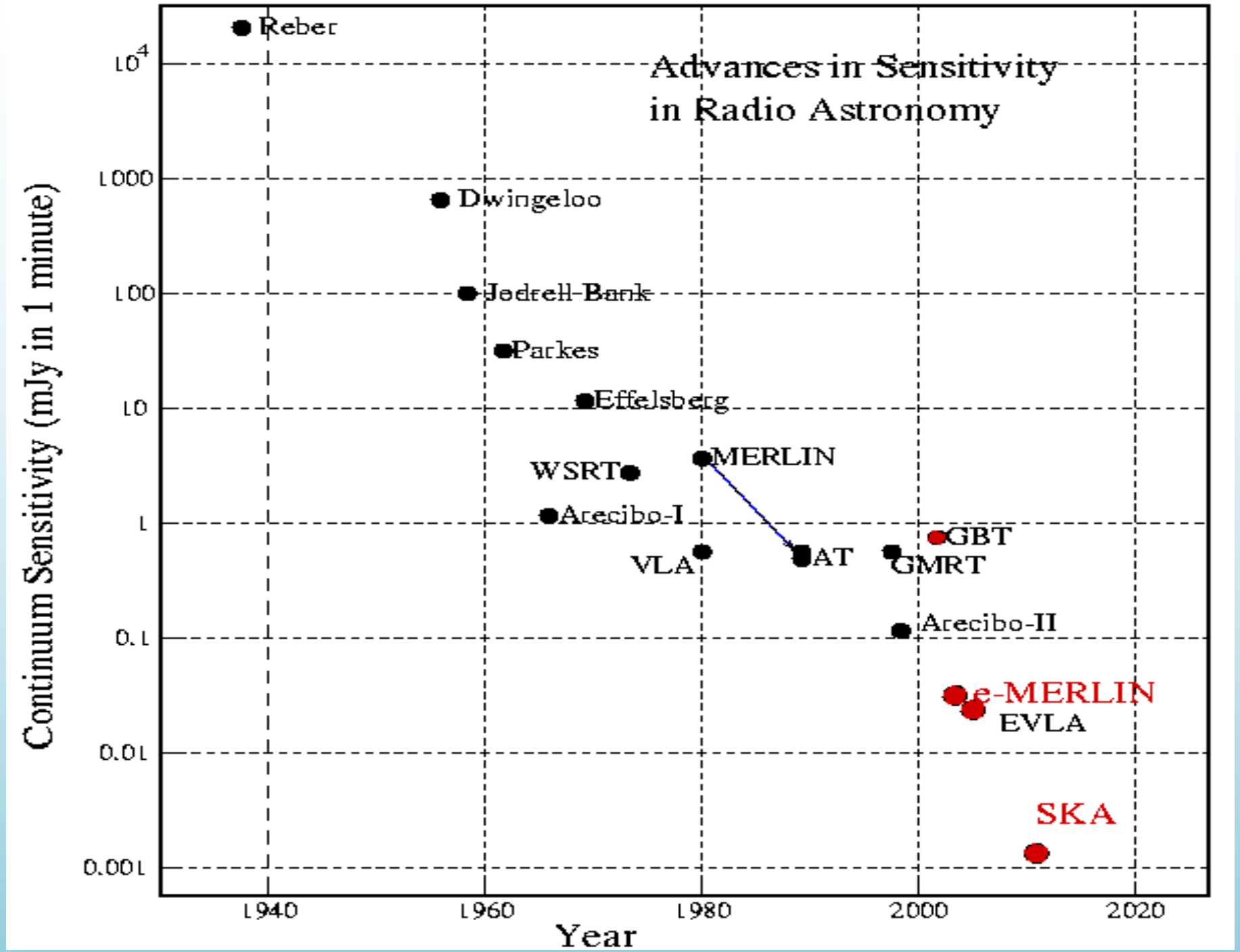
Advances in Sensitivity
in Radio Astronomy
Reber
Dwingeloo
Jodrell-Bank
Parkes
Effelsberg
WSRT
MERLIN
Arecibo-I
VLA
AT
GMRT
GBT
Arecibo-II
e-MERLIN
EVLA
SKA
Continuum Sensitivity (mJy in 1 minute)
Year
1940
1960
1980
2000
2020

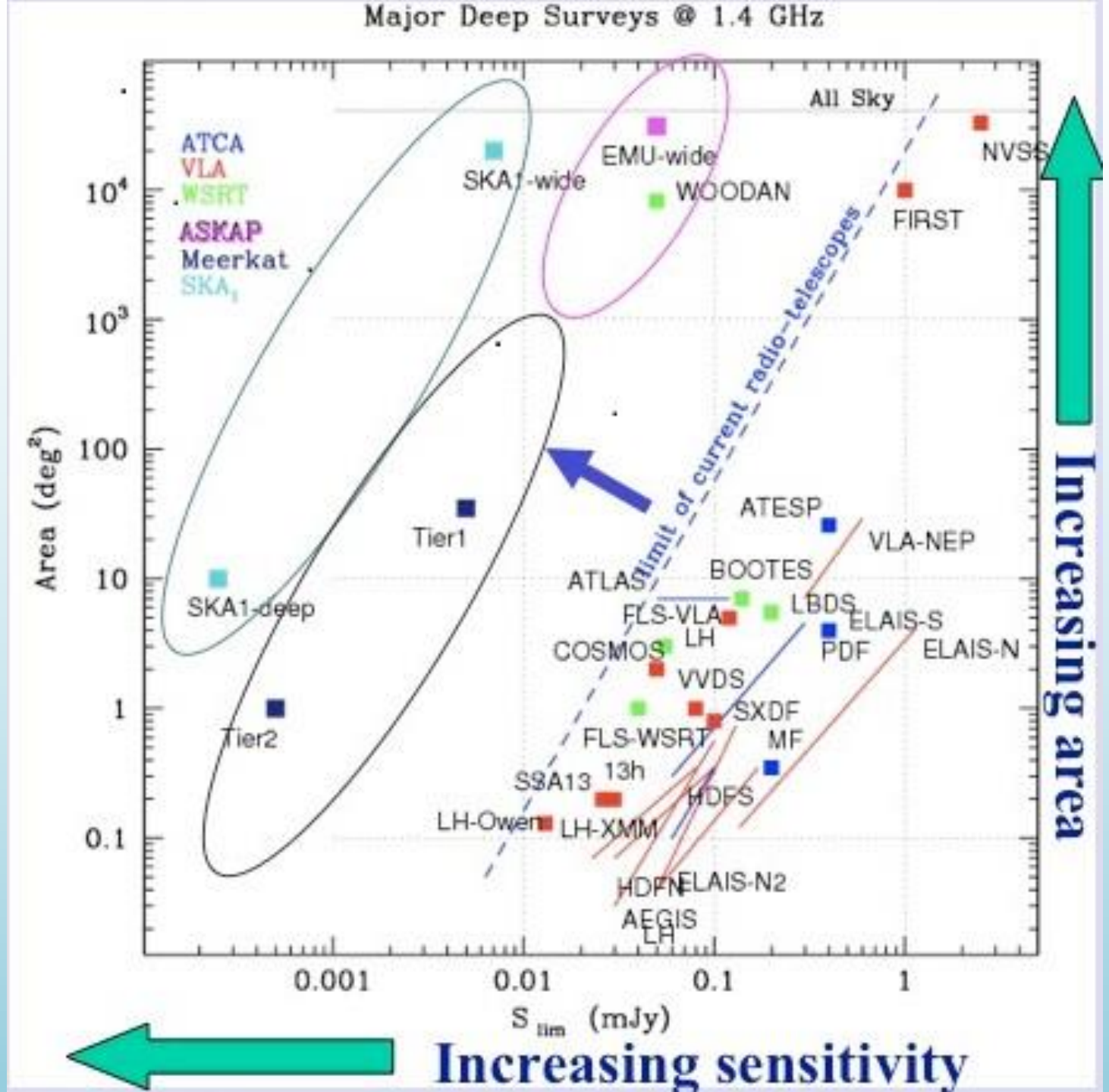
Major Deep Surveys @ 1.4 GHz
ATCA
VLA
WSRT
ASKAP
Meerkat
SKA1
All Sky
NVSS
FIRST
EMU-wide
WOODAN
SKA1-wide
Limit of current radio-telescopes
ATESP
VLA-NEP
BOOTES
ATLAS
LBDS
FLS-VLA
ELAIS-S
LH
COSMOS
PDF
ELAIS-N
VVDS
SXDF
FLS-WSRT
MF
13h
SSA13
HDFS
LH-Owen
LH-XMM
ELAIS-N2
HDFN
AEGIS
LH
Tier1
Tier2
SKA1-deep
Area (deg²)
S lim (mJy)
Increasing area
Increasing sensitivity

Resolution Comparison

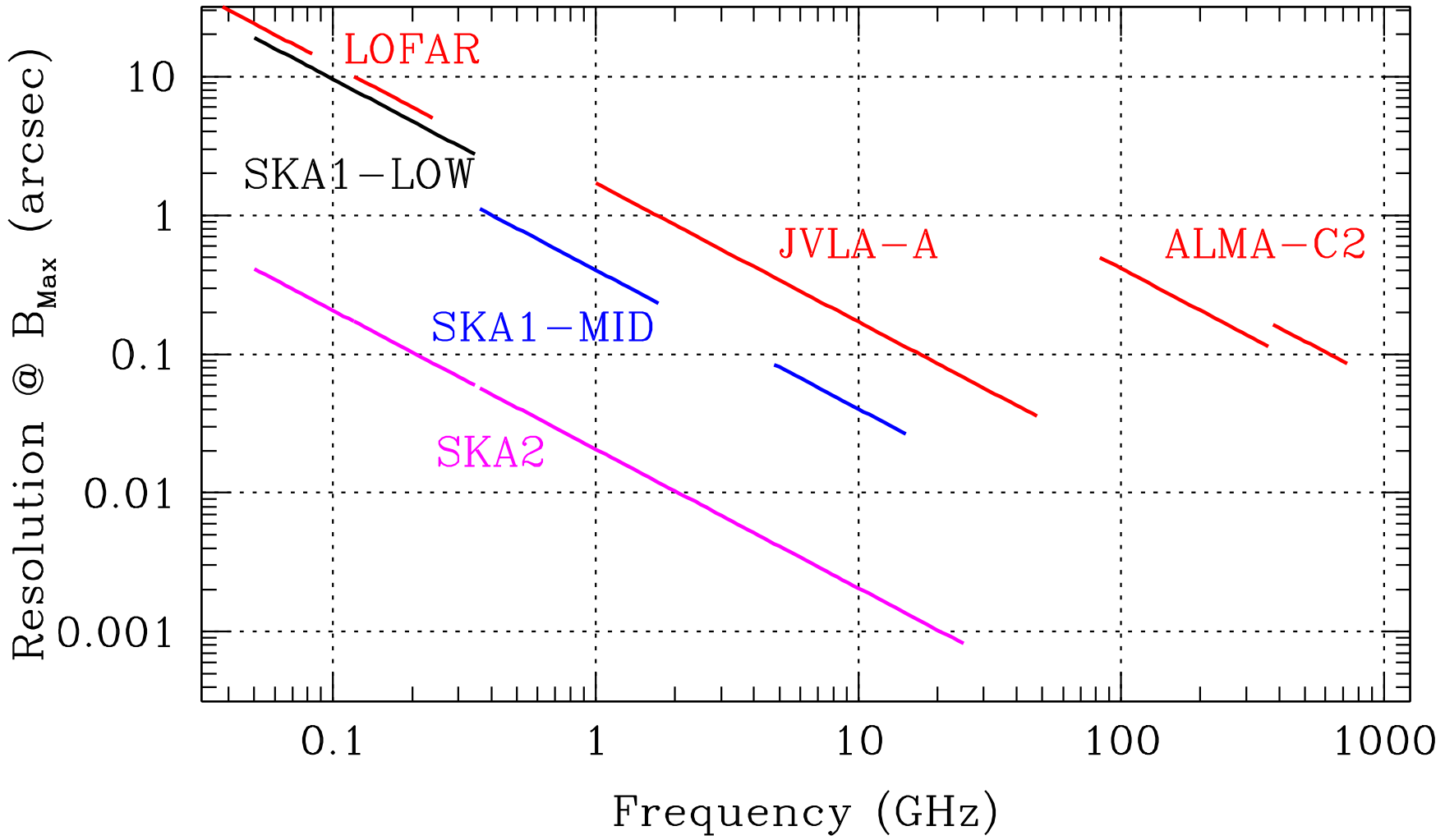

Galaxy HI Evolution:
out to z ~ 1 with SKA1 and z ~ 5 with SKA2

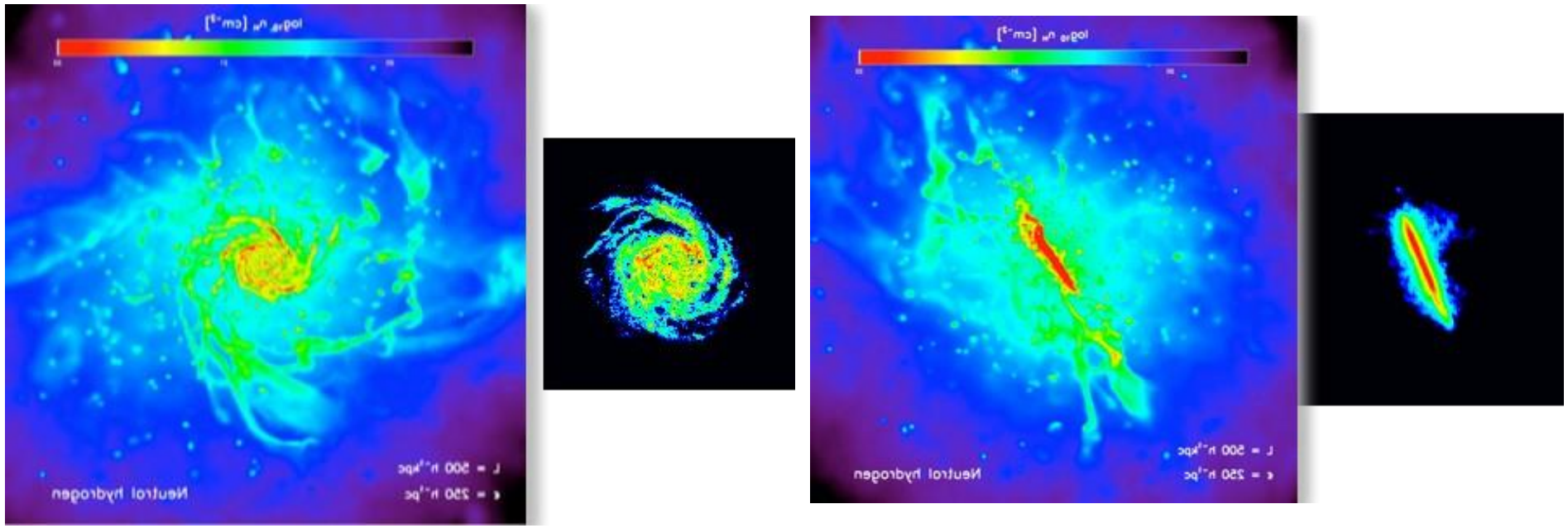

(Simulations: Schaye et al. 2010, Images: Oosterloo 2014)

- Understanding galaxy assembly and the baryon cycle
  - Determine the impact of galaxy environments
  - Probe gas inflow and removal, diffuse gas $N_{HI} < 10^{17}$ cm^{-2}
  - Measure angular momentum build-up

Galaxy/AGN Evolution – Modeling

Need of Fine-tuning source models

- Classical RL-AGNs
- SF gals.
- RQ-AGN
- Other classes?

Some Critical Issues for pathfinders/precursors:

- ev. of Low-P AGNs (Meerkat)
- extrapolation of local LF of SF & AGN to lower powers (ASKAP)

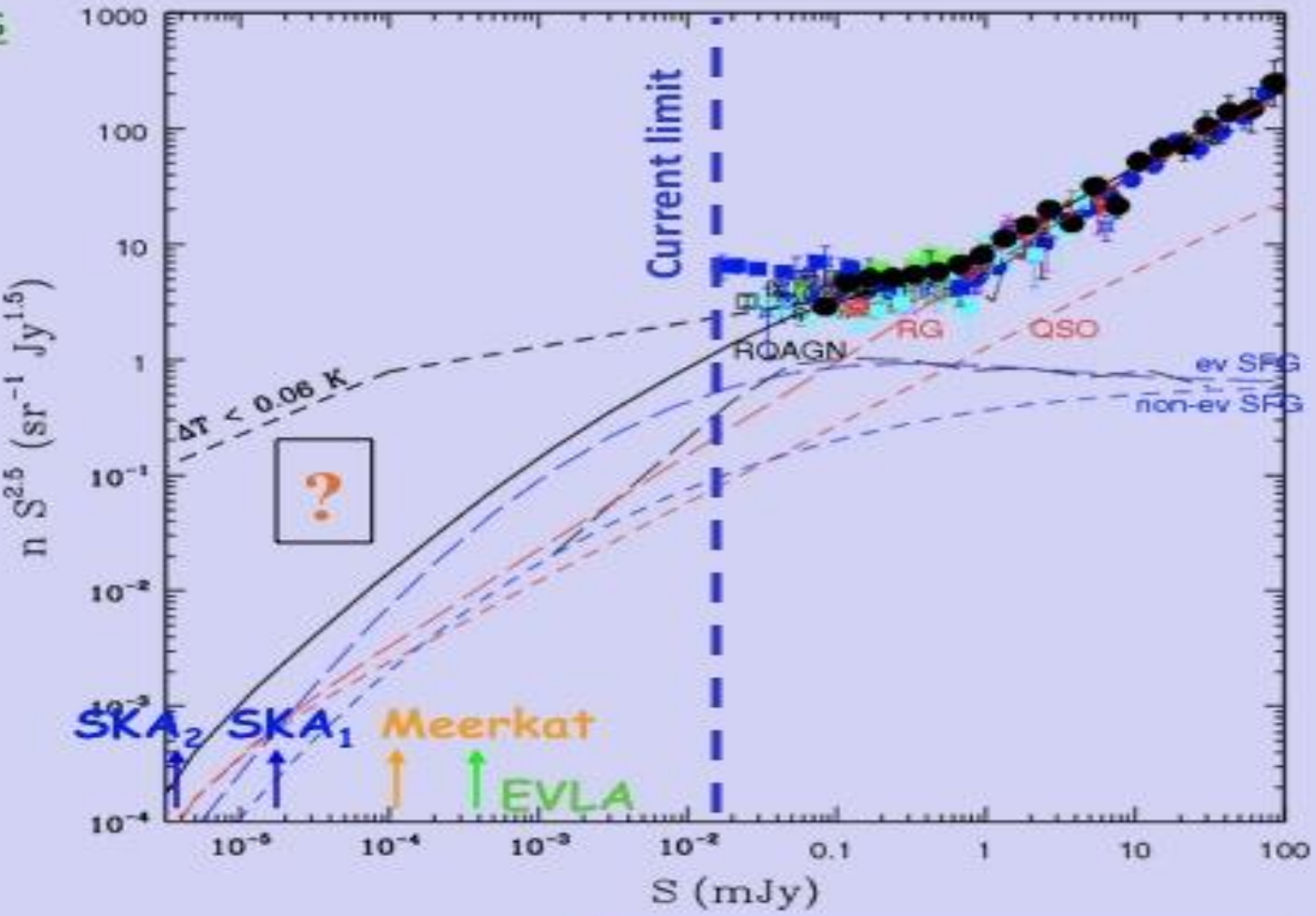

1.4 GHz Source Counts

Galaxy Evolution Studies in the Radio Continuum: Understanding the Star Formation History of the Universe

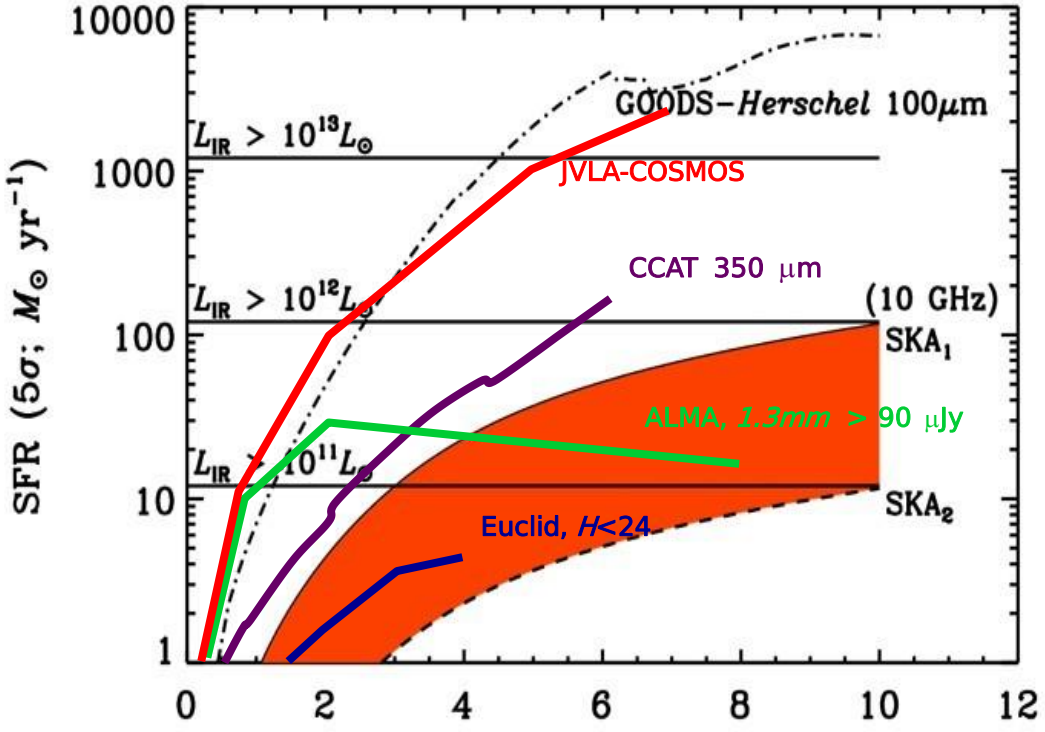

(Murphy et al. 2015)

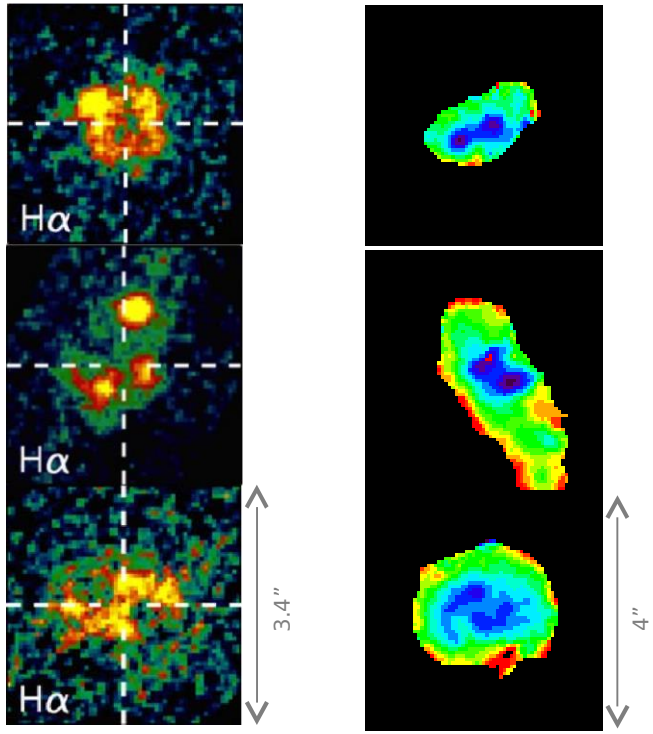

Wuyts et al 2013, **z~1** Cibinel et al 2014, **z~2**
Hα–based SFR-maps **UV-based** SFR-maps

- Unmatched sensitivity to star formation rates (10 $M_\odot$/yr) out to z ~ 4 with SKA1 and z ~ 10 with SKA2
- Resolved (sub-kpc) imaging of star forming disks out to z ~ 1 with SKA1 and z ~ 6 with SKA2

Conclusions

- So far, radio surveys have played only a marginal role in the study of the cosmic star formation history, but the SKA and, to some extent, its precursors will change this drastically, pushing the radio band at the forefront in terms of sensitivity to SFR in comparison to other bands
- SKA2 is expected to detect, with a 1,000 h exposure, a galaxy with a SFR ~ 10 $M_{\odot}$ up to $z \sim 8$ (Murphy et al. 2015), thus providing a more complete view of the cosmic star formation than any other forthcoming instrument.
- With 200 km baselines, observations at ~10 GHz will be able to achieve a maximum angular resolution ≤0″.03, sampling 250 pc scales within disk galaxies at $z \geq 1$, providing an extinction-free view for the morphologies of dusty star-bursting galaxies that dominate the star formation activity between $1 \leq z \leq 3$.
- While probing such fine physical scales requires sources that are extremely bright, the SKA should still have the sensitivity to easily resolve sub-L_* at high redshifts (Murphy et al. 2015; L_* galaxies at $1 \leq z \leq 3$ have corresponding total IR luminosities ranging between $10^{11}\ L_{\odot} \leq L_{IR} \leq 10^{12}\ L_{\odot}$). SKA1-MID will easily resolve such sources at $z \leq 2$, while also being able to map galaxies at 0″.1 resolution that are forming stars at 100 $M_{\odot}$ /yr.
- Such high resolution imaging will be well matched to that of JWST. Resolving highly obscured star-bursting systems at $z \geq 1$, with 500 pc resolution, will enable critical new investigations of their energetics and distinguish between disks and mergers without being subject to spatially varying obscuration of the rest frame UV light.